

# Predicting properties of hard-coating alloys using *ab-initio* and machine learning methods

H. Levämäki,<sup>1,\*</sup> F. Tasnadi,<sup>1</sup> D. G. Sangiovanni,<sup>1</sup> L. J. S. Johnson,<sup>2</sup> R. Armiento,<sup>1</sup> and I. A. Abrikosov<sup>1,3</sup>

<sup>1</sup>*Department of Physics, Chemistry and Biology,  
Linköping University, SE-581 83 Linköping, Sweden*

<sup>2</sup>*Sandvik Coromant, S-12680 Stockholm, Sweden*

<sup>3</sup>*Materials Modeling and Development Laboratory,*

*National University of Science and Technology 'MISIS', 119049 Moscow, Russia*

(Dated: November 24, 2021)

Accelerated design of novel hard coating materials requires state-of-the-art computational tools, which include data-driven techniques, building databases, and training machine learning models against the databases. In this work, we present a development of a heavily automated high-throughput workflow to build a database of industrially relevant hard coating materials, such as binary and ternary nitrides. We use Vienna Ab initio Simulation package as the density functional theory calculator and the high-throughput toolkit to automate the calculation workflow. We calculate and present results, including the elastic constants, one of the key materials parameter that determines mechanical properties of the coatings, for  $X_{1-x}Y_xN$  binary and ternary nitrides, where  $X, Y \in \{\text{Al, Ti, Zr, Hf}\}$  and fraction  $x = 0, \frac{1}{4}, \frac{1}{2}, \frac{3}{4}, 1$ . We explore ways for ML techniques to support and complement the designed databases. We find that the crystal graph convolutional neural network model trained on Materials Project data for ordered lattices has sufficient prediction accuracy for the disordered nitrides, suggesting that the existing databases provide important data for predicting mechanical properties of qualitatively different type of material systems, in our case hard coating alloys, not included in the original dataset.

## I. INTRODUCTION

Hard coating materials have a wide range of applications including metal cutting, scratch resistant coatings, grinding, and aerospace and automotive parts. For metal cutting tools, hard coatings are essential to their machining performance, increasing it by orders of magnitude over uncoated tools in most applications. Since the beginning, high-hardness materials have been developed experimentally, but for a few decades computational tools, such as density functional theory (DFT) [1, 2] and molecular dynamics, have been used to support and complement experiments. However, as the design of new coatings moves from binary and ternary systems to quaternary and beyond, the combinatorial complexity increases rapidly, making conventional approaches increasingly difficult.

More recently, machine learning (ML) has been found to be a viable way to reduce the number of experiments, as well as computations, to accelerate the design process [3–7]. Demand for robust ML models is there, but a big hurdle in their adoption is the limited availability of data, either experimental or computational, that ML models need to be trained on. Experimental data has traditionally been relatively scarce, while computational databases, such as Materials Project [8] and AFLOW [9], have grown to contain tens or hundreds of thousands of entries. For example, Avery *et al.* used AFLOW and a combined ML and evolutionary search method to predict

new superhard phases in carbon [6]. Mazhnik *et al.* used Materials Project data to train the crystal graph convolutional neural network (CGCNN) [10] model to predict the bulk and shear moduli of ordered compounds using only the structural and chemical information of the system as input [5], obtaining good results. In this paper we extend the approach to qualitatively different class of materials, disordered alloys (as deposited metastable thin films). It is well-known that ML is good at interpolation, but bad at extrapolation, and it is therefore vital to establish how well ML models extrapolate from ordered data to disordered data. We utilize a transfer learning (TL) approach [11] to predict polycrystalline elastic constants of disordered alloys based on data obtained from ordered compounds. To our knowledge, there are only very few TL studies in predicting properties of alloys. For a broad overview of ML approaches utilized in case of alloys, see [12].

From the point of view of practical applications, e.g., to design new hard coatings, however, currently existing databases are lacking for two reasons. Firstly, elastic constants are important: for instance, the intrinsic hardness of a material can be qualitatively assessed from the elastic constants and moduli [13, 14]. However, since elastic constants are demanding to calculate, only a limited fraction of the entries in existing databases have elastic constants data included. Secondly, most industrially relevant hard coatings, e.g.,  $\text{Ti}_{1-x}\text{Al}_x\text{N}$ ,  $\text{Cr}_{1-x}\text{Al}_x\text{N}$ , and  $\text{Ti}_{1-x}\text{Si}_x\text{N}$ , are substitutionally disordered [15], and are often thermodynamically metastable or even unstable, which is possible due to the far-from-equilibrium synthesis techniques of physical vapor deposition. Existing databases, on the other hand, are focused on ordered

---

\* [henrik.levamaki@liu.se](mailto:henrik.levamaki@liu.se)

Table I. Mean absolute error (MAE) in GPa (except the unitless Poisson's ratio  $\nu$ ) and mean absolute relative error (MARE)  $(X_{\text{rel}} - X_{\text{unrel}})/X_{\text{unrel}}$  in % between the relaxed and unrelaxed elastic properties.

	MAE								
	$c_{11}$	$c_{12}$	$c_{13}$	$c_{33}$	$c_{44}$	$B$	$G$	$E$	$\nu$
B1	8	6	—	—	9	4	4	10	0.004
B3	4	3	—	—	38	3	17	38	0.035
B4	41	34	39	108	11	3	26	57	0.052

	MARE								
	$c_{11}$	$c_{12}$	$c_{13}$	$c_{33}$	$c_{44}$	$B$	$G$	$E$	$\nu$
B1	2	5	—	—	6	2	3	3	2
B3	2	2	—	—	28	2	17	15	13
B4	12	31	46	32	14	2	26	23	21

compounds. Creating databases for disordered systems is therefore an activity that requires more attention. There is a recent effort to enable data-driven study of high-entropy ceramics [16], and in this paper we work towards a database of disordered hard coating materials. Because of significant computational costs, direct first-principles calculations for disordered alloys would lead to a relatively small database, which limits the amount of data to train ML models on. On the other hand, there are recent efforts in literature to find ways to make ML useful for small datasets [11, 17–20].

Given the abundance of data for ordered compounds, we investigate how ordered data can help with the lack of disordered data. Using a bigger data set to help the modeling of a smaller data set is one of the goals of TL [18]. In this paper we use a TL approach, in which the CGCNN model is trained on the data for ordered compounds available in Materials Project, and the model is then used to predict the properties of disordered systems. We are interested in predicting quantities that are known to correlate with the intrinsic hardness of materials, such as bulk and shear moduli [21–24]. We find that even without an explicit inclusion of the data for disordered alloys in the model, it is able to predict the bulk and shear moduli of the industrially relevant nitrides with sufficient accuracy.

## II. RESULTS

### A. DFT results

We calculate disordered binary and ternary nitrides of the form  $X_{1-x}Y_xN$ , where  $X,Y \in \{\text{Al, Ti, Zr, Hf}\}$  and the concentration parameter  $x = 0, \frac{1}{4}, \frac{1}{2}, \frac{3}{4}, 1$ . The calculations are performed with and without taking atomic relaxations into account, so that we can assess the importance of the atomic relaxation effects. Cell shape and volume are optimized in both cases. Note that in this comparison in the unrelaxed B4 calculations we must fix the one available atomic degree of freedom along the  $z$ -

Table II. Calculated DFT elastic constants, bulk ( $B$ ), shear ( $G$ ) and Young's moduli ( $E$ ) in GPa, as well as Poisson's ratio ( $\nu$ ). The SB column refers to the Strukturbericht designation. Those B4 systems that relaxed into the  $B_k$  structure are marked by “B4 →  $B_k$ ” in the SB column.

Alloy	SB	$c_{11}$	$c_{12}$	$c_{13}$	$c_{33}$	$c_{44}$	$B$	$G$	$E$	$\nu$
AlN	B1	432	167	—	—	307	256	219	511	0.167
HfN	B1	598	112	—	—	129	274	166	414	0.248
Hf <sub>0.75</sub> Al <sub>0.25</sub> N	B1	524	124	—	—	147	258	166	410	0.235
Hf <sub>0.50</sub> Al <sub>0.50</sub> N	B1	460	142	—	—	174	248	168	411	0.224
Hf <sub>0.25</sub> Al <sub>0.75</sub> N	B1	429	158	—	—	221	248	182	439	0.205
Hf <sub>0.75</sub> Ti <sub>0.25</sub> N	B1	581	113	—	—	134	269	168	417	0.242
Hf <sub>0.50</sub> Ti <sub>0.50</sub> N	B1	567	119	—	—	142	268	171	423	0.237
Hf <sub>0.25</sub> Ti <sub>0.75</sub> N	B1	577	122	—	—	153	274	180	443	0.231
Hf <sub>0.75</sub> Zr <sub>0.25</sub> N	B1	584	109	—	—	128	267	165	410	0.244
Hf <sub>0.50</sub> Zr <sub>0.50</sub> N	B1	569	108	—	—	128	262	162	403	0.244
Hf <sub>0.25</sub> Zr <sub>0.75</sub> N	B1	554	107	—	—	127	256	159	395	0.243
TiN	B1	584	136	—	—	166	285	187	460	0.231
Ti <sub>0.75</sub> Al <sub>0.25</sub> N	B1	535	139	—	—	181	271	187	456	0.22
Ti <sub>0.50</sub> Al <sub>0.50</sub> N	B1	492	155	—	—	214	268	194	469	0.208
Ti <sub>0.25</sub> Al <sub>0.75</sub> N	B1	443	161	—	—	250	255	199	474	0.19
ZrN	B1	544	110	—	—	125	255	156	389	0.246
Zr <sub>0.75</sub> Al <sub>0.25</sub> N	B1	477	124	—	—	139	242	153	379	0.239
Zr <sub>0.50</sub> Al <sub>0.50</sub> N	B1	427	141	—	—	166	236	156	384	0.229
Zr <sub>0.25</sub> Al <sub>0.75</sub> N	B1	411	157	—	—	215	242	174	421	0.21
Zr <sub>0.75</sub> Ti <sub>0.25</sub> N	B1	538	111	—	—	130	253	159	394	0.24
Zr <sub>0.50</sub> Ti <sub>0.50</sub> N	B1	540	116	—	—	138	257	164	406	0.237
Zr <sub>0.25</sub> Ti <sub>0.75</sub> N	B1	568	122	—	—	150	271	176	434	0.233
AlN	B3	285	152	—	—	178	196	120	299	0.246
HfN	B3	292	152	—	—	93	199	83	219	0.317
Hf <sub>0.75</sub> Al <sub>0.25</sub> N	B3	274	144	—	—	100	188	84	219	0.306
Hf <sub>0.50</sub> Al <sub>0.50</sub> N	B3	261	144	—	—	106	183	84	219	0.301
Hf <sub>0.25</sub> Al <sub>0.75</sub> N	B3	263	144	—	—	127	183	94	241	0.281
Hf <sub>0.75</sub> Ti <sub>0.25</sub> N	B3	287	150	—	—	93	196	82	216	0.316
Hf <sub>0.50</sub> Ti <sub>0.50</sub> N	B3	286	150	—	—	92	195	82	216	0.316
Hf <sub>0.25</sub> Ti <sub>0.75</sub> N	B3	289	152	—	—	92	198	82	216	0.318
Hf <sub>0.75</sub> Zr <sub>0.25</sub> N	B3	281	148	—	—	91	193	80	211	0.318
Hf <sub>0.50</sub> Zr <sub>0.50</sub> N	B3	272	147	—	—	90	189	78	206	0.319
Hf <sub>0.25</sub> Zr <sub>0.75</sub> N	B3	263	144	—	—	88	184	75	198	0.321
TiN	B3	293	155	—	—	91	201	81	214	0.322
Ti <sub>0.75</sub> Al <sub>0.25</sub> N	B3	282	154	—	—	103	197	85	223	0.311
Ti <sub>0.50</sub> Al <sub>0.50</sub> N	B3	274	154	—	—	116	194	89	232	0.301
Ti <sub>0.25</sub> Al <sub>0.75</sub> N	B3	271	153	—	—	138	192	98	251	0.282
ZrN	B3	258	144	—	—	87	182	73	193	0.323
Zr <sub>0.75</sub> Al <sub>0.25</sub> N	B3	247	140	—	—	92	176	74	195	0.316
Zr <sub>0.50</sub> Al <sub>0.50</sub> N	B3	240	142	—	—	98	175	74	195	0.315
Zr <sub>0.25</sub> Al <sub>0.75</sub> N	B3	253	146	—	—	123	182	88	227	0.292
Zr <sub>0.75</sub> Ti <sub>0.25</sub> N	B3	262	144	—	—	87	184	74	196	0.323
Zr <sub>0.50</sub> Ti <sub>0.50</sub> N	B3	269	148	—	—	88	188	76	201	0.322
Zr <sub>0.25</sub> Ti <sub>0.75</sub> N	B3	282	154	—	—	89	197	78	207	0.325
AlN	B4	376	129	98	352	112	194	121	301	0.242
HfN	B4	253	161	162	220	47	188	44	122	0.391
Hf <sub>0.75</sub> Al <sub>0.25</sub> N	B4 → B <sub>k</sub>	296	204	113	359	107	201	79	210	0.326
Hf <sub>0.50</sub> Al <sub>0.50</sub> N	B4 → B <sub>k</sub>	298	176	145	110	109	135	51	136	0.332
Hf <sub>0.25</sub> Al <sub>0.75</sub> N	B4	305	140	124	216	87	175	79	206	0.304
Hf <sub>0.75</sub> Ti <sub>0.25</sub> N	B4 → B <sub>k</sub>	298	210	106	493	113	214	85	225	0.325
Hf <sub>0.50</sub> Ti <sub>0.50</sub> N	B4 → B <sub>k</sub>	304	210	103	491	120	214	90	237	0.316
Hf <sub>0.25</sub> Ti <sub>0.75</sub> N	B4 → B <sub>k</sub>	311	212	106	500	128	218	94	247	0.311
Hf <sub>0.75</sub> Zr <sub>0.25</sub> N	B4 → B <sub>k</sub>	292	211	105	495	106	212	81	216	0.331
Hf <sub>0.50</sub> Zr <sub>0.50</sub> N	B4 → B <sub>k</sub>	288	206	102	483	107	208	81	215	0.328
Hf <sub>0.25</sub> Zr <sub>0.75</sub> N	B4 → B <sub>k</sub>	286	201	101	470	107	205	82	217	0.324
TiN	B4 → B <sub>k</sub>	322	219	111	524	138	227	100	262	0.308
Ti <sub>0.75</sub> Al <sub>0.25</sub> N	B4 → B <sub>k</sub>	311	212	120	438	138	218	93	244	0.313
Ti <sub>0.50</sub> Al <sub>0.50</sub> N	B4 → B <sub>k</sub>	314	196	128	363	148	211	98	255	0.299
Ti <sub>0.25</sub> Al <sub>0.75</sub> N	B4	315	136	136	214	88	181	80	209	0.307
ZrN	B4 → B <sub>k</sub>	284	195	101	458	106	202	82	217	0.321
Zr <sub>0.75</sub> Al <sub>0.25</sub> N	B4 → B <sub>k</sub>	277	195	108	320	101	188	72	192	0.33
Zr <sub>0.50</sub> Al <sub>0.50</sub> N	B4 → B <sub>k</sub>	287	177	125	202	110	176	74	195	0.316
Zr <sub>0.25</sub> Al <sub>0.75</sub> N	B4	302	147	122	190	89	169	76	198	0.304
Zr <sub>0.75</sub> Ti <sub>0.25</sub> N	B4 → B <sub>k</sub>	288	200	101	453	110	203	83	219	0.32
Zr <sub>0.50</sub> Ti <sub>0.50</sub> N	B4 → B <sub>k</sub>	297	205	102	461	116	207	87	229	0.316
Zr <sub>0.25</sub> Ti <sub>0.75</sub> N	B4 → B <sub>k</sub>	307	210	105	485	125	215	92	242	0.313

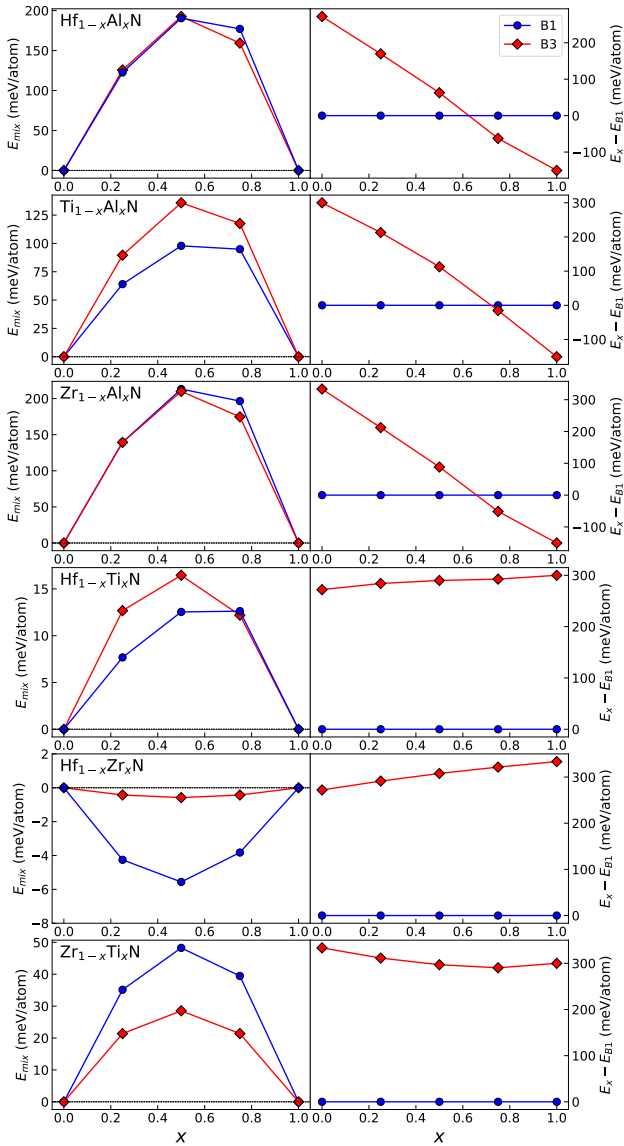


Figure 1. Left panel: calculated DFT mixing energies  $E[X_{1-x}Y_xN] - (1-x)E[XN] - xE[YN]$ . Right panel: structural stability with respect to B1 with the same composition  $E[\text{structure}] - E[B1]$ . B4 alloys, most of which relaxed into the  $B_k$  setting (see Table II) are not shown.

direction. We fix it by setting the atomic unit cell coordinates as  $z_1 = 0$  and  $z_2 = 0.38$  in terms of the notation of Ref. [25]. One can define  $z_1 = 0$  without loss of generality and  $z_2 = 0.38$  represents the average value for the type of systems we consider here. It should be noted that the  $z_2$  coordinate is also called the “ $u$  parameter” in some literature sources [26].

Let us first investigate the effect of atomic relaxations on the elastic constants. Assessment of the computational cost due to atomic relaxation is useful, because computing the elastic constants is time consuming. Thus,

if the effect is minor, some computational time could be saved by neglecting atomic relaxations. Several previous studies have investigated the impact that atomic relaxations have on the elastic constant results [27–33]. In summary, the previous studies have found that, in most cases, relaxed and unrelaxed elastic constants are quite similar. Most often, the relative differences are lower than  $\approx 10\%$ . Relaxation effects can also be qualitatively estimated from symmetry arguments. For some lattice symmetries, a uniform deformation (used for elastic-constant calculations) may be sufficient to shift atoms from their equilibrium positions. This implies, in turn, that the resulting elastic tensors strongly depend on the strain matrix used for the calculation.

Table I shows the mean absolute errors (MAE) and mean absolute relative errors (MARE) ( $X_{\text{rel}} - X_{\text{unrel}})/X_{\text{unrel}}$ ) between the relaxed and unrelaxed elastic constants and the polycrystalline quantities, calculated for all the alloys that can be found in Table II, except for those that are marked “B4  $\rightarrow B_k$ ”. We have not included those B4 structures that relaxed into  $B_k$ , because all unrelaxed calculations remain in the B4 phase and therefore are not directly comparable to the relaxed calculations that end up in the  $B_k$  phase (see Fig. 3). We can see that for the B1, which is a highly symmetric structure, relaxation effects are minor. With the B3 phase, atomic relaxation effects on calculated  $c_{11}$  and  $c_{12}$  are negligible. Conversely, the MAE and MARE values indicate a strong effect of atomic relaxation on  $c_{44}$ . That is due to local B3-symmetry-breaking induced by shear lattice distortions. Also the B4 phase shows noticeable relaxation effects.

Based on our findings, if one is only interested in the bulk modulus, one might perform only unrelaxed calculations. If the shear modulus, or quantities that depend on the shear modulus, is of interest, the unrelaxed shear modulus will be accurate only for structures such as B1, where the different distortions do not break the symmetry in such a way that there are significant distortion dependent atomic movements.

The calculated elastic properties are shown in Table II and the mixing energies  $E[X_{1-x}Y_xN] - (1-x)E[XN] - xE[YN]$  and relative stabilities  $E[\text{structure}] - E[B1]$  of the B1 and B3 structure types are shown in Fig. 1. The B4 alloys, most of which relaxed into the  $B_k$  setting are not shown. All of the calculated alloys are found to be mechanically stable within a 10% tolerance of  $\epsilon = 1.1$  (see Sec. IV A). Dynamical stability checks, which are based on phonon dispersion calculations, are out of the scope of this work, but based on existing literature some of the calculated alloys can be expected to be dynamically unstable. All two-component systems are ordered and those systems have been checked against available Materials Project data and the two sets have been found to be generally in good agreement. Our results for the well-studied Ti<sub>1-x</sub>Al<sub>x</sub>N system are also in agreement with literature data [15, 34–36].

For the alloys in B1 structure we find good agreement

with the elastic constants, bulk modulus, and mixing energy results of Refs. [37, 38]. Ref. [37] calculated the same set of alloys that can be found in Fig. 1, except for  $\text{Hf}_{1-x}\text{Zr}_x\text{N}$ . The mixing energies of Fig. 1 are in general in good agreement with those of Ref. [37], except for the trend that Fig. 1 obtained mixing energies that are highly symmetrical in terms of the concentration parameter  $x$  axis. Our mixing energies in Fig. 1 show more pronounced asymmetry (except  $\text{Hf}_{1-x}\text{Zr}_x\text{N}$  and  $\text{Zr}_{1-x}\text{Ti}_x\text{N}$ ) with the  $x \approx 1$  side having larger positive mixing energies. The reason for these different trends could be related to differences in the SQS supercells between our study and Ref. [37].

We notice that all alloys, except  $\text{HfN}$  and Al-rich alloys, prefer the planar  $B_k$  structure. We interpret the tendency to relax toward the planar  $B_k$  structure ( $u$  parameter  $\sim 0.5$ ) as an effect induced by the dynamical instability (imaginary phonon frequencies [39], see Fig. 3g in Ref. [40]) combined with an energetic preference for the  $B_k$  hexagonal polymorph [41]. Additionally, the  $B4$   $\text{ZrN}$  and  $\text{HfN}$  binaries are predicted to be dynamically stable in the  $B_k$  phase [40].

Previous *ab initio* results [41] and Fig. 1 suggest that  $X_{1-x}\text{Al}_x\text{N}$  ( $X = \text{Ti}, \text{Zr}, \text{Hf}$ ) solid solutions energetically favor the  $B1$  structure for Al contents  $x \lesssim 0.5$ , whereas the wurtzite  $B4$  alloy phase becomes the most stable for high  $x$  ( $\gtrsim 0.7$ ). At ambient conditions, the ordered  $\text{TiN}$ ,  $\text{HfN}$ , and  $\text{ZrN}$  favor the  $B1$  structure, which is also their ground state. Other recent *ab initio* results indicate that  $\text{TiN}$  can be metastable in the  $B4$  structure (see Fig. 3g in Ref. [40]). Our calculations, however, do not find  $\text{TiN}$  to be stable in the  $B4$  structure. Note, indeed, that Ref. [40] reports phonon dispersion results only along a few high-symmetry directions. Evaluation of the  $B4$   $\text{TiN}$  phonon-density of states may be necessary to reveal imaginary frequencies.

## B. Machine learning results

Given that it is relatively resource heavy to calculate the elastic tensor of disordered structures, a large amount of supercomputer time would be needed to amass a sizable database of such materials. We are therefore interested in different strategies to supplement or augment the database using ML techniques. One way to tackle the problem of low data availability is to train the ML model to a part of the available data that is related to the problem at hand, and then appropriately modifying and verifying the model with the smaller dataset. This is the basic idea behind TL [18]. In this work we use an approach that might be considered a zeroth-order approximation to TL. In this approach we train an ML model using Materials Project data, which are ordered compounds, and see how well that model predicts the disordered alloys simulated in the present study. In other words, we check how well the patterns learned from the ordered dataset, without modifications, transfer or generalize to the dis-

Table III. The MAE (in GPa) and MARE (in %) for the test set and the disordered nitrides set. The  $B1+B3$  means the combination of the  $B1$  and  $B3$  structure sets.

MAE	<i>B</i>	<i>G</i>
test set	11.6	9.0
<u>disordered nitrides</u>		
unrelaxed $B1$	15.8	28.3
unrelaxed $B3$	3.9	23.6
unrelaxed $B1+B3$	9.7	25.9
relaxed $B1$	14.0	23.9
relaxed $B3$	5.3	7.9
relaxed $B1+B3$	9.5	15.7
MARE	<i>B</i>	<i>G</i>
test set	18.4	21.7
<u>disordered nitrides</u>		
unrelaxed $B1$	6.0	16.4
unrelaxed $B3$	2.1	23.7
unrelaxed $B1+B3$	4.0	20.2
relaxed $B1$	5.3	13.9
relaxed $B3$	2.9	9.8
relaxed $B1+B3$	4.1	11.8

ordered dataset. If the ML model generalizes well, one can employ the network to predict, or at least estimate the properties of disordered systems outright, as the case may be, or use it as a basis for further training with the disordered dataset [11]. Performing more sophisticated TL, such as fine-tuning and layer freezing [11, 18], is out of the scope of this study and will be addressed in future work.

Throughout the ML section, the  $B4$  phase is not included because most of the studied  $B4$  alloys turns out to be unstable and transform into  $B_k$  structure upon structural relaxation. At the same time, information on compounds with  $B_k$  structure in the databases is insufficient to build reliable ML models: hexagonal systems (and the  $B_k$  in particular) are underrepresented in the training set (only  $\sim 1000$  compounds are hexagonal out of the total 8000). One may view the inability to describe  $B4/B_k$  alloys as a limitation of the applicability of the ML and TL that requires further in-depth study. Additionally, those ordered binary compounds (concentration parameter  $x = 0$  or 1) that can be found in the Materials Project data are excluded, because for those data points the error would be biased as they were part of the training set.

The ML architecture that we use is the CGCNN, and Mazhnik *et al.* have shown that it can be successfully harnessed, together with Materials Project data, to predict simultaneously both the bulk and shear moduli of an input crystal structure. One could always train separate ML models for the bulk and shear moduli, but in the approach of Mazhnik *et al.* both quantities are treated on equal footing. Based on their good results, we are encour-

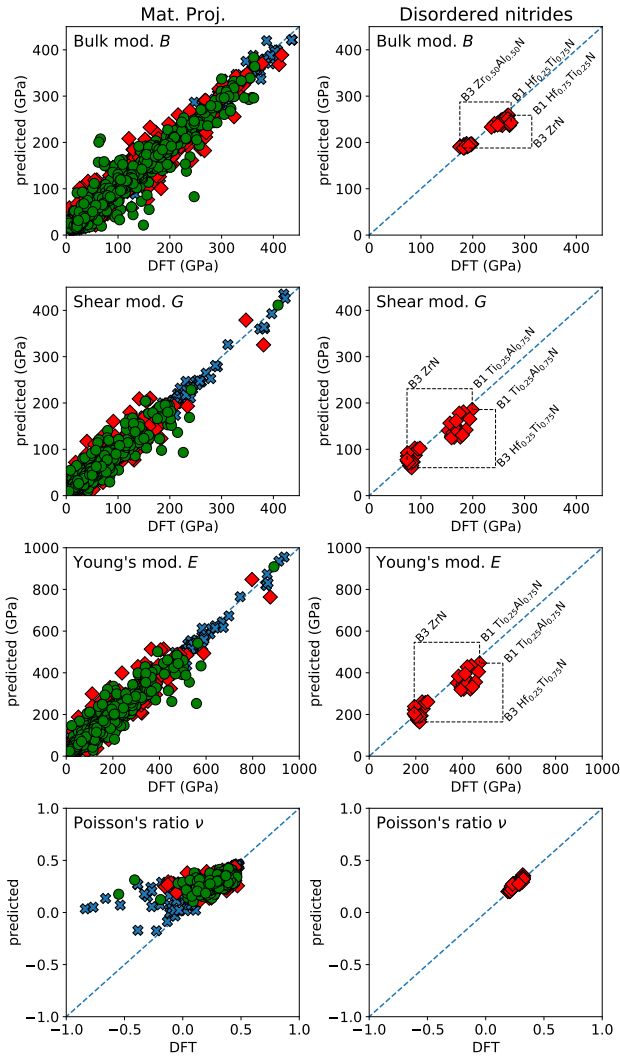


Figure 2. Parity plot of the DFT and ML predicted results. The dashed diagonal line indicates perfect agreement. In the Mat. Proj. column blue cross markers indicate training set, red diamonds validation set, and green disks test set. The minimum and maximum DFT and ML prediction values for the disordered nitrides are also labeled.

aged to implement a similar approach here. We employ a typical train-validate-test workflow to build the optimal CGCNN model from the Materials Project data.

The performance of the finished model is depicted in Table III in terms of MAE and MARE for the test set and the disordered dataset, with and without atomic relaxations. In the Table, the B1+B3 means the combination of the B1 and B3 structure sets. Table III shows that the predictions made by the ML model for the disordered alloys with B1 and B3 crystal structure are quite accurate, even though no actual TL was done to the model. We notice that for the B3 structures the shear modulus prediction error is noticeably better for the relaxed data

compared to unrelaxed data. This difference reflects the differences in unrelaxed and relaxed shear moduli in Table I. There are two possible reasons that could explain this behavior. Firstly, the ML prediction error is smaller for the relaxed data, which makes sense since the model was trained on Materials Project data, for which atomic relaxation is used systematically. It is reasonable to assume that the bonding lengths of the unrelaxed structures appear unphysical to the ML model. That would explain why the model performs poorly for unrelaxed structures. Secondly, the CGCNN construction includes a certain cutoff parameter (8 Å in this work) that is used to make the descriptor of each atomic site finite; neighboring atomic sites that fall outside the cutoff radius are neglected. When the structure is relaxed, some atomic sites may move beyond the cutoff radius while others may move within the radius. The descriptors between relaxed and unrelaxed structures are therefore slightly different, which could create discrepancies in the ML results for relaxed and unrelaxed structures.

An interesting observation is that the test set and disordered nitrides MAEs show opposite qualitative trends; for the test set, the shear modulus MAE is smaller than the bulk modulus MAE, while for the disordered data this trend is reversed. Overall, the average ML prediction error for the disordered nitrides is good for the bulk modulus and somewhat worse for the shear modulus. We can say that the CGCNN architecture generalizes quite well from ordered systems to disordered ones even without explicit fine-tuning of the ML model.

To get a clearer picture of the performance of the ML model, Fig. 2 shows a parity plot of the DFT versus ML predicted values (B4/B<sub>k</sub> not included). The left side of Fig. 2 shows the performance of the network for the test set (green round markers), as well as for the training set (blue cross markers). The figure also shows ML predictions for Young's modulus  $E$  and Poisson's ratio  $\nu$ , which are not directly produced by the ML model, but can be calculated from the predicted bulk and shear moduli. Our results for the test set are similar to those of Mazhnik *et al.* [5]. The prediction accuracy for the disordered nitrides falls within the accuracy range of the Materials Project test set.

The right column of the figure shows how well the ML model with the lowest loss function performs for the disordered nitrides. We can see a fairly tight clustering around the diagonal and an absence of major outliers. Clear outliers or significant scatter for the nitrides is not expected anyway, because the disordered dataset is very homogeneous (in terms of the variety of structures and chemical elements) compared to the Materials Project training set, so the ML model should work similarly for all the data points the disordered data. We can identify some structure specific trends in the ML prediction accuracy. While the bulk and shear moduli of the B3 structures are especially well predicted, the B1 shear moduli show a lower accuracy. For the B1 phase the shear modulus is consistently underestimated and the largest single

underestimation is  $\approx 50$  GPa. It is not easy to give a simple reason for the inconsistent shear modulus prediction performance, but we can note that the shear modulus, as evidenced by Table I, is a more sensitive quantity than the bulk modulus. It is the aim of future studies to see how much fine-tuning the current ML network will improve the prediction accuracy.

### III. DISCUSSION

We have developed an automated high-throughput workflow for building a computational database of disordered hard-coating materials and presented results of our calculations. The reliability of our data is verified by comparing to the Materials Project data and existing literature. Moreover, we have trained the CGCNN ML model on ordered compounds from the Materials Project and demonstrated that this model is able to readily predict the bulk and shear moduli of disordered nitrides with sufficient accuracy. The CGCNN architecture seems to be able to learn such fundamental patterns in the data that these patterns hold regardless of the degree of order, indicating good generalizability of CGCNN from ordered to disordered systems. Prediction accuracy for disordered systems can be further improved by using the ML model trained on ordered data as the starting point for TL. Our findings open new ways to gain insight into disordered hard coating materials, as well as to support and possibly speed up the investigations of disordered hard coating materials, which are computationally demanding to calculate and thus slow to accumulate into a large database.

## IV. METHODS

### A. DFT calculations

The DFT calculations were performed using the Vienna Ab initio Simulation Package (VASP) [42, 43]. The exchange and correlation effects were treated at the generalized gradient approximation (GGA) level [44–46] using the Perdew-Burke-Ernzerhof (PBE) [47] functional. Energy cutoff is set to 500 eV in the preliminary relaxation phase and to 700 eV in subsequent phases. The precision mode is set to Accurate (PREC=Accurate). The Gaussian smearing scheme with a smearing width of 0.05 eV is used. Ionic relaxations are stopped when all forces are below the threshold 0.01 eV/Å. In cases where the threshold 0.01 eV/Å is difficult to reach, the threshold is increased to 0.03 eV/Å or 0.05 eV/Å. The elastic constants calculations include the support grid for augmentation charges (ADDGRID=.TRUE.).

The VASP calculations were managed with The High-Throughput Toolkit (*httk*) [48, 49]. The *httk* software offers workflows to create input files, manage calculations

on computing clusters, automatically fix broken calculations by adjusting VASP input settings, and organize results in databases. The automatic computation of elastic constants is implemented in *httk*.

In this work we consider disordered binary and ternary nitrides in cubic rocksalt (B1) [50], cubic zincblende (B3) [51], and hexagonal wurtzite (B4) [25] structures. These structure types are illustrated in Fig. 3. Disorder is modeled using the special quasirandom structures (SQS) technique [52, 53]. The SQS supercell that are used in this study are listed in Supplementary materials. Here, substitutional disorder is considered only on the metallic sublattice, i.e., the nitrogen sublattice is ordered because it is fully occupied by nitrogen atoms. All SQS supercells had size of 96 atoms. This size has been found to be within optimal range for ternary nitrides from the standpoint of accuracy versus computational speed [35]. The B1  $X_{0.5}Y_{0.5}N$  SQS cell is taken from the supplementary materials of Ref. [35], where it is referred to as the “(4×4×3)” cell. In Ref. [35] the “(4×4×3)” cell was found to model disorder at a high-quality level, that is, comparable to SQS cells of bigger sizes. The B3  $X_{0.5}Y_{0.5}N$  SQS can be easily derived from the B1  $X_{0.5}Y_{0.5}N$  SQS by noting that the B1 conventional unit cell turns into B3 when the N atom is shifted from the high-symmetry position  $\frac{1}{2}\vec{a}_1 + \frac{1}{2}\vec{a}_2 + \frac{1}{2}\vec{a}_3$  to another high-symmetry position  $\frac{1}{4}\vec{a}_1 + \frac{1}{4}\vec{a}_2 + \frac{1}{4}\vec{a}_3$ . All the other SQS supercells are generated with the stochastic Monte-Carlo SQS program mcsqs [54], which is part of the Alloy Theoretic Automated Toolkit (ATAT) program package [55].

Although the SQS scheme is an efficient way to simulate disorder, the downside is that the proper (macroscopic) symmetry is broken and the generated SQS cells typically only have triclinic symmetry. For the calculation of elastic constants this poses a problem, because we are interested in elastic constant tensors of cubic (B1 and B3) or hexagonal (B4) classes instead of triclinic-structure elastic tensors. In order to derive properly symmetrized elastic constants from the full triclinic elastic tensor, we employ the projection technique that has been discussed in Ref. [35] and references therein. The “unprojected” triclinic elastic constants are reported in the Supplementary materials. We can see that the deviations between the different crystallographic directions are small, even though the disordered SQS supercells do not respect the proper macroscopic symmetry. As Ref. [35] shows, the projected elastic constants have the desirable property that they converge fast to the “correct” value as a function of supercell size, faster than the unprojected elastic constants. To facilitate automated calculations, we have implemented the symmetrization technique in *httk*. The elastic constants in VASP are calculated using the stress-strain method in the same general way that was used, e.g., in Ref. [56]. Four distorted structures are generated for each strain component (in terms of Voigt notation) and the range of distortion are  $-3\%$ ,  $-1.5\%$ ,  $1.5\%$ ,  $3\%$  for non-shear components and  $-6\%$ ,  $-3\%$ ,  $3\%$ ,  $6\%$  for shear components. All polycrystalline quantities

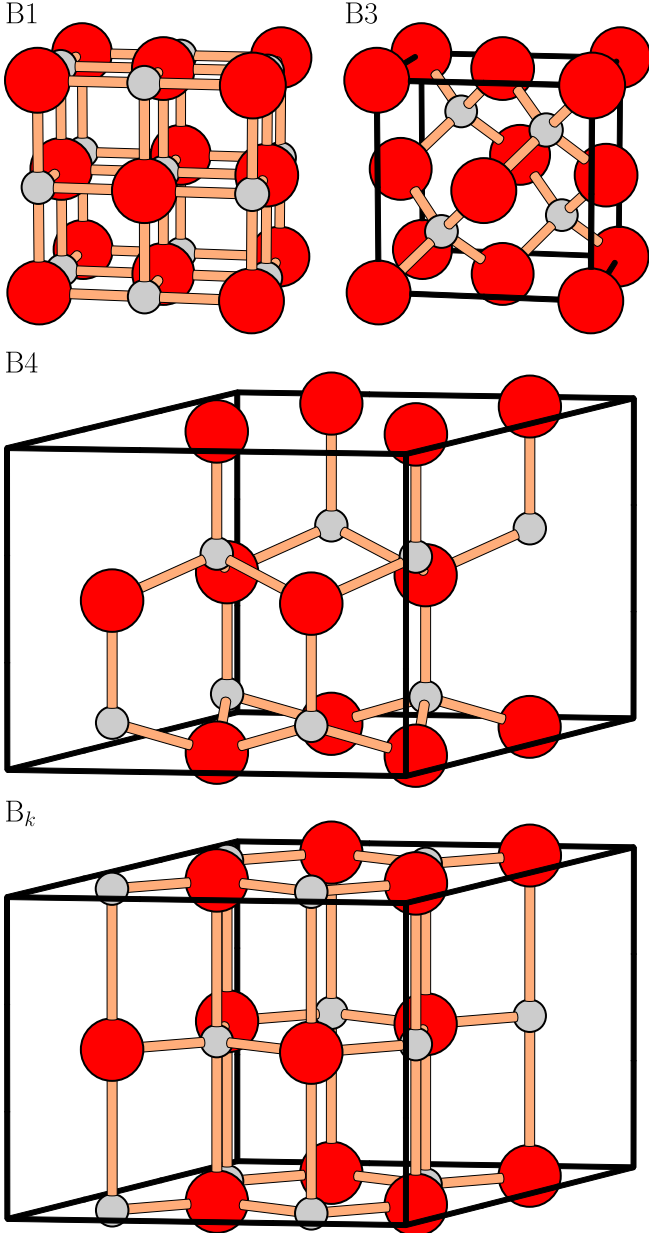


Figure 3. The different structures considered in this work. The larger red spheres indicate metallic sublattice and the smaller gray spheres nitrogen sublattice.

are calculated using the Hill averaging scheme [56]. The mechanical stability is checked based on the Born-Huang stability criteria [57]. In addition to the normal stability check, we also use the stricter tolerance based check of Ref. [56]. For example, cubic systems must fulfill a condition  $C_{11} > |C_{12}|$  to be mechanically stable. In the tolerance based check, a more rigorous condition  $C_{11} > \epsilon |C_{12}|$  ( $\epsilon > 1$ ) must be fulfilled. All of the calculated alloys are found to be mechanically stable. Dynamical stability checks, which are based on phonon dispersion calcula-

tions, are out of the scope of this work, but based on existing literature some of the calculated alloys can be expected to be dynamically unstable.

## B. Machine learning

The ML part of this work is done using the PyTorch package. The CGCNN [10] architecture is applied using the code available at GitHub as the basis [58]. In the CGCNN model the input crystal structure is transformed into a crystal graph, which is constructed from node feature vectors  $\mathbf{v}_i$  and edge feature vectors  $\mathbf{u}_{ij}$ . The node feature vector encodes information about the type of atom located at atomic site  $i$ . The atomic information is encoded in an integer vector using one-hot or dummy encoding. For example, if the training data includes elements N, Al, and Ti, then the elements can be encoded as N  $\Rightarrow$  [1, 0, 0], Al  $\Rightarrow$  [0, 1, 0], and Ti  $\Rightarrow$  [0, 0, 1]. The edge feature vector encodes information about the bonds that the atom at site  $i$  makes with its nearest neighbours. This bonding information is encoded by discretizing a Gaussian distribution function centered around the nearest neighbours of the reference site  $i$ . The feature vector for site  $i$  with one of its nearest neighbours  $j$  is then calculated as

$$\mathbf{u}_{ij} = \exp\left(-\frac{(d_{ij} - \alpha)^2}{h^2}\right), \quad (1)$$

where  $d_{ij}$  is the distance between sites  $i$  and  $j$ ,  $h$  is a discretization step size, and  $\alpha$  is a vector of discretized trial distances

$$\alpha = [0, h, 2h, 3h, \dots, R_{\text{cut}}], \quad (2)$$

where  $R_{\text{cut}}$  is a cutoff radius to make the vector finite in length. We can see that when  $\alpha$  is close to  $d_{ij}$ ,  $\mathbf{u}_{ij}$  has values close to one, and when  $\alpha$  deviates from  $d_{ij}$ ,  $\mathbf{u}_{ij}$  is close to zero. The crystal graph is then fed into a convolutional neural network, which consists of convolutional layers and pooling layers. The convolutional layers iteratively modify the node feature vector of site  $i$  by convolving it with the edge feature vector  $\mathbf{u}_{ij}$  and node feature vectors of surrounding sites  $j$ . The convolution is described by the equation

$$\begin{aligned} \mathbf{v}_i^{(t+1)} = & \mathbf{v}_i^{(t)} + \sum_j \sigma\left(\mathbf{z}_{i,j}^{(t)} \mathbf{W}_f^{(t)} + \mathbf{b}_f^{(t)}\right) \\ & \odot g\left(\mathbf{z}_{i,j}^{(t)} \mathbf{W}_s^{(t)} + \mathbf{b}_s^{(t)}\right), \end{aligned} \quad (3)$$

where  $\mathbf{z}_{i,j}^{(t)} = \mathbf{v}_i^{(t)} \oplus \mathbf{v}_j^{(t)} \oplus \mathbf{u}_{i,j}$  is the concatenation of the node and edge feature vectors,  $\sigma$  is the sigmoid activation function,  $g$  is the softplus activation function, and  $\mathbf{W}_s^{(t)}, \mathbf{W}_f^{(t)}, \mathbf{b}_s^{(t)}, \mathbf{b}_f^{(t)}$  are the weights and biases of the  $t$ th convolutional layer [10]. After  $R$  convolutional layers (three in this work), a pooling layer is applied to produce

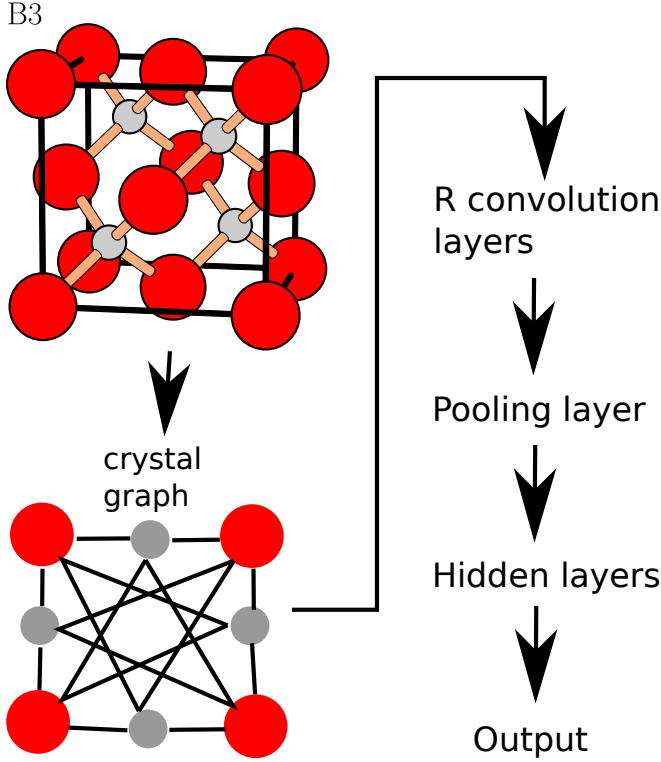


Figure 4. Diagram of the CGCNN architecture.

the overall feature vector of the crystal  $\mathbf{v}_c$ . The pooling layer is implemented as a normalized summation of all the feature vectors  $\mathbf{v}_1^{(0)}, \mathbf{v}_2^{(0)}, \dots, \mathbf{v}_1^{(R)}, \mathbf{v}_2^{(R)}, \dots, \mathbf{v}_N^{(R)}$ . Finally,  $\mathbf{v}_c$  is inputted to fully connected hidden layers (two in this work) that predict the output. A diagram of the CGCNN architecture is presented in Fig. 4.

Following Ref. [5], the network is trained to predict bulk and shear moduli using Materials Project data as the training and test datasets. At the time of writing, Materials Project contains a little over 8000 systems that have elasticity data available. We randomly split the data into training, validation, and test sets in a 8:1:1 ratio. While the training set is used to optimize the model parameters, the difference between the validation and test has to do with avoiding biases in the final estimation of the accuracy of the ML model. Here validation set is used to minimize overfitting in a way that is described below. This means that the validation set is part of the model optimization process and the model accuracy for the validation set is slightly biased. Hence we need a test set that only contains data that the final ML model has never seen before. By evaluating model performance on the test set is therefore a way to minimize biases and maximize the trustworthiness of the model accuracy estimate.

Before training, the target values (bulk and shear mod-

uli) are normalized using the formula

$$\tilde{\mathbf{y}} = \frac{\mathbf{y} - \bar{\mathbf{y}}}{\sigma(\mathbf{y})}, \quad (4)$$

where  $\bar{\mathbf{y}}$  is the mean and  $\sigma(\mathbf{y})$  is the standard deviation of the target vector  $\mathbf{y}$ . The loss function to be minimized is defined in terms of the normalized bulk modulus  $\tilde{\mathbf{B}}$  and shear modulus  $\tilde{\mathbf{G}}$  as

$$\mathcal{L} = \frac{\sum_i (\tilde{B}_i^{\text{pred}} - \tilde{B}_i^{\text{DFT}})^2 + (\tilde{G}_i^{\text{pred}} - \tilde{G}_i^{\text{DFT}})^2}{N}, \quad (5)$$

where  $N$  is the number of data points. Based on the information of Refs. [5, 10, 18] and their supplementary materials, as well as our own testing, we can infer reasonable values for the hyperparameters without performing extensive hyperparameter tuning. The crystal structure descriptor related settings are the same as those reported in Ref. [5]. The training process uses the Adam optimizer with a learning rate of 0.005 and weight decay 0.0. Training is continued for a minimum of 500 epochs to give the randomly initialized model parameters enough time to develop. Training is stopped after 1500 epochs, as it is unlikely that any significant progress will happen after that point. In order to avoid the training process getting stuck in a suboptimal local minimum, 30 instances were trained. To reduce random variance, an ensemble of five networks with the lowest validation loss is used to make predictions. The validation set is used to decide the final model parameters by extracting the parameters from the epoch that yields the loss function minimum for the validation set. This is one form of the early stopping technique and the purpose is to mitigate overfitting issues [59]. Finally, an unbiased estimate of the performance of the finished model is obtained by evaluating the model using the unseen test set (see Table III). For further details about the CGCNN architecture and the training process, the reader is referred to Refs. [5, 10, 18].

## V. DATA AVAILABILITY

Relevant calculated DFT data and instructions to download the Materials Project data, as well as the trained ML model to reproduce the results of this paper are provided as Supplementary materials.

## VI. CODE AVAILABILITY

The code to reproduce the results of this paper are provided as Supplementary materials.

## VII. ACKNOWLEDGMENTS

We gratefully acknowledge financial support from the Competence Center Functional Nanoscale Materials

(FunMat-II) (Vinnova Grant No. 2016–05156). Support from the Knut and Alice Wallenberg Foundation (Wallenberg Scholar Grant No. KAW-2018.0194), the Swedish Government Strategic Research Areas in Materials Science on Functional Materials at Linköping University (Faculty Grant SFO-Mat-LiU No. 2009 00971) and SeRC is gratefully acknowledged. Theoretical analysis of results of first-principles calculations was supported by the Russian Science Foundation (Project No. 18-12-00492). R.A. acknowledges support from the Swedish Research Council (VR) Grant No. 2020-05402 and the Swedish e-Science Centre (SeRC). The computations were enabled by resources provided by the Swedish National Infrastructure for Computing (SNIC), partially funded by the Swedish Research Council through grant agreement no.

2018-05973. The computational resources provided by the PDC Center for High Performance Computing are also acknowledged.

## VIII. COMPETING INTERESTS

The authors declare no competing interests.

## IX. AUTHOR CONTRIBUTIONS

H.L., R.A., and I.A.A. conceived the project. H.L. performed the calculations and analyzed the results. H.L., F.T., D.G.S., L.J.S.J., R.A., and I.A.A. discussed the results and wrote the manuscript.

- 
- [1] P. Hohenberg and W. Kohn, *Phys. Rev.* **136**, B864 (1964).
- [2] W. Kohn and L. J. Sham, *Phys. Rev.* **140**, A1133 (1965).
- [3] H. Bhadeshia, *ISIJ International* **39**, 966 (1999).
- [4] A. M. Tehrani, A. O. Oliynyk, M. Parry, Z. Rizvi, S. Couper, F. Lin, L. Miyagi, T. D. Sparks, and J. Brugoch, *Journal of the American Chemical Society* **140**, 9844 (2018).
- [5] E. Mazhnik and A. R. Oganov, *Journal of Applied Physics* **128**, 075102 (2020).
- [6] P. Avery, X. Wang, C. Oses, E. Gossett, D. M. Proserpio, C. Toher, S. Curtarolo, and E. Zurek, *npj Computational Materials* **5**, 10.1038/s41524-019-0226-8 (2019).
- [7] E. Bedolla, L. C. Padíerna, and R. Castañeda-Priego, *Journal of Physics: Condensed Matter* **33**, 053001 (2020).
- [8] A. Jain, S. P. Ong, G. Hautier, W. Chen, W. D. Richards, S. Dacek, S. Cholia, D. Gunter, D. Skinner, G. Ceder, and K. A. Persson, *APL Materials* **1**, 011002 (2013).
- [9] S. Curtarolo, W. Setyawan, S. Wang, J. Xue, K. Yang, R. H. Taylor, L. J. Nelson, G. L. Hart, S. Sanvito, M. Buongiorno-Nardelli, N. Mingo, and O. Levy, *Computational Materials Science* **58**, 227 (2012).
- [10] T. Xie and J. C. Grossman, *Physical Review Letters* **120**, 145301 (2018).
- [11] H. Yamada, C. Liu, S. Wu, Y. Koyama, S. Ju, J. Shiomi, J. Morikawa, and R. Yoshida, *ACS Central Science* **5**, 1717 (2019).
- [12] G. L. W. Hart, T. Mueller, C. Toher, and S. Curtarolo, *Nature Reviews Materials* **6**, 730 (2021).
- [13] J. S. Tse, *Journal of Superhard Materials* **32**, 177 (2010).
- [14] A. M. Tehrani and J. Brugoch, *Journal of Solid State Chemistry* **271**, 47 (2019).
- [15] I. A. Abrikosov, A. Knutsson, B. Alling, F. Tasnádi, H. Lind, L. Hultman, and M. Odén, *Materials* **4**, 1599 (2011).
- [16] C. Oses, C. Toher, and S. Curtarolo, *Nature Reviews Materials* **5**, 295 (2020).
- [17] P.-P. D. Breuck, G. Hautier, and G.-M. Rignanese, arXiv <http://arxiv.org/abs/2004.14766v1>.
- [18] J. Lee and R. Asahi, *Computational Materials Science* **190**, 110314 (2021).
- [19] Y. Zhang and C. Ling, *npj Computational Materials* **4**, 10.1038/s41524-018-0081-z (2018).
- [20] C. Chen, Y. Zuo, W. Ye, X. Li, and S. P. Ong, *Nature Computational Science* **1**, 46 (2021).
- [21] A. R. Oganov and A. O. Lyakhov, *Journal of Superhard Materials* **32**, 143 (2010).
- [22] Y. Tian, B. Xu, and Z. Zhao, *International Journal of Refractory Metals and Hard Materials* **33**, 93 (2012).
- [23] A. G. Kvashnin, Z. Allahyari, and A. R. Oganov, *Journal of Applied Physics* **126**, 040901 (2019).
- [24] E. Mazhnik and A. R. Oganov, *Journal of Applied Physics* **126**, 125109 (2019).
- [25] M. J. Mehl, D. Hicks, C. Toher, O. Levy, R. M. Hanson, G. L. W. Hart, and S. Curtarolo, *Prototype of B4 structure* (accessed February 24, 2021).
- [26] E. H. Kisi and M. M. Elcombe, *Acta Crystallographica Section C Crystal Structure Communications* **45**, 1867 (1989).
- [27] L.-Y. Tian, Q.-M. Hu, R. Yang, J. Zhao, B. Johansson, and L. Vitos, *Journal of Physics: Condensed Matter* **27**, 315702 (2015).
- [28] L.-Y. Tian, G. Wang, J. S. Harris, D. L. Irving, J. Zhao, and L. Vitos, *Materials & Design* 10.1016/j.matdes.2016.11.079 (2016).
- [29] H. Song, F. Tian, Q.-M. Hu, L. Vitos, Y. Wang, J. Shen, and N. Chen, *Physical Review Materials* **1**, 023404 (2017).
- [30] L.-Y. Tian, L.-H. Ye, Q.-M. Hu, S. Lu, J. Zhao, and L. Vitos, *Computational Materials Science* **128**, 302 (2017).
- [31] G. Kim, H. Diao, C. Lee, A. Samaei, T. Phan, M. de Jong, K. An, D. Ma, P. K. Liaw, and W. Chen, *Acta Materialia* **181**, 124 (2019).
- [32] M. Jafary-Zadeh, K. H. Khoo, R. Laskowski, P. S. Brancio, and A. V. Shapeev, *Journal of Alloys and Compounds* **803**, 1054 (2019).
- [33] a. Taga, L. Vitos, B. Johansson, and G. Grimvall, *Physical Review B* **71**, 014201 (2005).
- [34] H. Lind, R. Forsén, B. Alling, N. Ghafoor, F. Tasnádi, M. P. Johansson, I. A. Abrikosov, and M. Odén, *Applied Physics Letters* **99**, 091903 (2011).
- [35] F. Tasnádi, M. Odén, and I. A. Abrikosov, *Phys. Rev. B* **85**, 144112 (2012).

- [36] N. Shulumba, O. Hellman, L. Rogström, Z. Raza, F. Tasnádi, I. A. Abrikosov, and M. Odén, *Applied Physics Letters* **107**, 231901 (2015).
- [37] D. Holec, L. Zhou, R. Rachbauer, and P. H. Mayrhofer, *Journal of Applied Physics* **113**, 113510 (2013).
- [38] F. Wang, D. Holec, M. Odén, F. Mücklich, I. A. Abrikosov, and F. Tasnádi, *Acta Materialia* **127**, 124 (2017).
- [39] E. I. Isaev, S. I. Simak, I. A. Abrikosov, R. Ahuja, Y. K. Vekilov, M. I. Katsnelson, A. I. Lichtenstein, and B. Johansson, *Journal of Applied Physics* **101**, 123519 (2007).
- [40] M. Arango-Ramirez, A. Vargas-Calderon, and A. M. Garay-Tapia, *Journal of Applied Physics* **128**, 105106 (2020).
- [41] D. Holec, R. Rachbauer, L. Chen, L. Wang, D. Luef, and P. H. Mayrhofer, *Surface and Coatings Technology* **206**, 1698 (2011).
- [42] G. Kresse and J. Furthmüller, *Comput. Mater. Sci.* **6**, 15 (1996).
- [43] G. Kresse and J. Furthmüller, *Phys. Rev. B* **54**, 11169 (1996).
- [44] D. C. Langreth and M. J. Mehl, *Phys. Rev. B* **28**, 1809 (1983).
- [45] J. P. Perdew, *Physical Review Letters* **55**, 1665 (1985).
- [46] J. P. Perdew and W. Yue, *Physical Review B* **33**, 8800 (1986).
- [47] J. P. Perdew, K. Burke, and M. Ernzerhof, *Physical Review Letters* **77**, 3865 (1996).
- [48] R. Armiento, *The High-Throughput Toolkit (httk)* (accessed February 23, 2021).
- [49] R. Armiento, in *Machine Learning Meets Quantum Physics* (Springer International Publishing, 2020) pp. 377–395.
- [50] M. J. Mehl, D. Hicks, C. Toher, O. Levy, R. M. Hanson, G. L. W. Hart, and S. Curtarolo, *Prototype of B1 structure* (accessed February 24, 2021).
- [51] M. J. Mehl, D. Hicks, C. Toher, O. Levy, R. M. Hanson, G. L. W. Hart, and S. Curtarolo, *Prototype of B3 structure* (accessed February 24, 2021).
- [52] A. Zunger, S.-H. Wei, L. G. Ferreira, and J. E. Bernard, *Physical Review Letters* **65**, 353 (1990).
- [53] S. H. Wei, L. G. Ferreira, J. E. Bernard, and A. Zunger, *Physical Review B* **42**, 9622 (1990).
- [54] A. Van De Walle, P. Tiwary, M. De Jong, D. L. Olmsted, M. Asta, A. Dick, D. Shin, Y. Wang, L. Q. Chen, and Z. K. Liu, *Calphad: Computer Coupling of Phase Diagrams and Thermochemistry* **42**, 13 (2013).
- [55] a. Van de Walle, M. Asta, G. Ceder, and G. Cederb, *Calphad Comput. Coupling Phase Diagrams Thermochem.* **26**, 539 (2002).
- [56] M. D. Jong, W. Chen, T. Angsten, A. Jain, R. Notestine, A. Gamst, M. Sluiter, C. K. Ande, S. V. D. Zwaag, J. J. Plata, C. Toher, S. Curtarolo, G. Ceder, K. a. Persson, and M. Asta, *Scientific Data* **2**, 150009 (2015).
- [57] F. Mouhat and F.-X. Coudert, *Physical Review B* **90**, 224104 (2014).
- [58] T. Xie, <https://github.com/txie-93/cgcnn> (accessed April 22, 2021).
- [59] T. Hastie, R. Tibshirani, and J. Friedman, *The Elements of Statistical Learning* (Springer New York, 2009).

**Supplementary:  
Predicting properties of hard-coating alloys using *ab-initio* and machine learning  
methods**

H. Levämäki,<sup>1,\*</sup> F. Tasnadi,<sup>1</sup> D. G. Sangiovanni,<sup>1</sup> L. J. S. Johnson,<sup>2</sup> R. Armiento,<sup>1</sup> and I. A. Abrikosov<sup>1,3</sup>

<sup>1</sup>*Department of Physics, Chemistry and Biology,  
Linköping University, SE-581 83 Linköping, Sweden*

<sup>2</sup>*Sandvik Coromant, S-12680 Stockholm, Sweden*

<sup>3</sup>*Materials Modeling and Development Laboratory,  
National University of Science and Technology 'MISIS', 119049 Moscow, Russia*

(Dated: November 23, 2021)

---

\* [henrik.levamaki@liu.se](mailto:henrik.levamaki@liu.se)

## I. ELASTIC CONSTANTS

### A. Unrelaxed calculations

Table I: Elastic constants of the unrelaxed B1 calculations before projection to the proper symmetry.

Alloy	SB	$c_{11}$	$c_{22}$	$c_{33}$	$c_{12}$	$c_{13}$	$c_{23}$	$c_{44}$	$c_{55}$	$c_{66}$	$c_{14}$	$c_{15}$	$c_{16}$	$c_{24}$	$c_{25}$	$c_{26}$	$c_{34}$	$c_{35}$	$c_{36}$	$c_{45}$	$c_{46}$	$c_{56}$
AlN	B1	440	433	431	173	172	168	308	308	308	0	0	0	0	0	0	0	0	0	0	0	0
HfN	B1	595	609	595	110	121	110	127	131	127	-4	-1	3	1	3	1	3	-1	-4	-1	1	-1
$\text{Hf}_{0.75}\text{Al}_{0.25}\text{N}$	B1	530	524	537	120	111	121	133	136	127	1	4	2	-3	-1	1	-1	3	3	2	3	-2
$\text{Hf}_{0.50}\text{Al}_{0.50}\text{N}$	B1	478	455	478	128	119	128	141	157	144	-2	5	-1	5	1	-5	3	6	0	0	6	-1
$\text{Hf}_{0.25}\text{Al}_{0.75}\text{N}$	B1	433	446	441	146	138	141	185	184	182	2	7	4	-4	0	3	-3	6	-3	-1	-1	1
$\text{Hf}_{0.75}\text{Ti}_{0.25}\text{N}$	B1	589	598	589	106	117	107	137	139	136	-2	0	2	0	0	1	0	0	-2	0	-1	-1
$\text{Hf}_{0.50}\text{Ti}_{0.50}\text{N}$	B1	579	594	578	108	118	106	145	149	145	-2	1	1	0	-1	2	0	1	-2	0	-1	0
$\text{Hf}_{0.25}\text{Ti}_{0.75}\text{N}$	B1	598	600	597	117	126	118	155	159	155	0	2	1	0	0	1	0	2	0	1	-2	1
$\text{Hf}_{0.75}\text{Zr}_{0.25}\text{N}$	B1	579	591	579	105	115	105	127	130	127	-3	0	2	0	3	0	2	0	-3	-1	0	-1
$\text{Hf}_{0.50}\text{Zr}_{0.50}\text{N}$	B1	569	578	568	109	119	109	126	129	126	-3	-1	2	0	1	0	1	-1	-3	-1	0	-1
$\text{Hf}_{0.25}\text{Zr}_{0.75}\text{N}$	B1	551	561	551	106	114	106	126	128	126	-2	0	1	0	2	0	1	0	-2	-1	0	-1
TiN	B1	575	583	579	131	138	128	165	165	165	1	3	-1	1	-7	1	0	3	2	3	-3	3
$\text{Ti}_{0.75}\text{Al}_{0.25}\text{N}$	B1	534	530	540	138	136	140	177	178	173	0	0	1	0	0	1	-1	2	-1	1	2	0
$\text{Ti}_{0.50}\text{Al}_{0.50}\text{N}$	B1	489	467	494	147	143	151	203	211	201	-2	4	0	3	0	-3	1	3	4	0	1	0
$\text{Ti}_{0.25}\text{Al}_{0.75}\text{N}$	B1	454	457	472	162	160	162	242	240	240	2	4	2	-1	-2	1	-2	5	-4	-1	-2	1
ZrN	B1	544	553	544	110	118	110	124	126	124	-2	-1	1	0	0	0	1	-1	-2	-1	0	-1
$\text{Zr}_{0.75}\text{Al}_{0.25}\text{N}$	B1	487	484	493	120	112	119	128	131	123	0	0	3	-5	-4	4	-3	1	4	2	2	-1
$\text{Zr}_{0.50}\text{Al}_{0.50}\text{N}$	B1	444	420	443	128	121	129	138	153	140	-2	3	0	4	1	-5	3	5	0	0	5	0
$\text{Zr}_{0.25}\text{Al}_{0.75}\text{N}$	B1	412	420	421	145	140	138	183	182	181	1	5	5	-3	-2	3	-4	5	-3	-1	-1	0
$\text{Zr}_{0.75}\text{Ti}_{0.25}\text{N}$	B1	539	547	538	105	114	105	131	133	131	0	2	-1	2	1	-1	2	2	-4	0	-1	0
$\text{Zr}_{0.50}\text{Ti}_{0.50}\text{N}$	B1	547	556	547	110	121	109	139	142	139	-1	0	1	1	-2	2	1	0	-2	0	-2	0
$\text{Zr}_{0.25}\text{Ti}_{0.75}\text{N}$	B1	575	579	574	119	128	120	151	154	151	-1	1	1	0	-1	1	0	1	-1	0	-3	0

Table II: Elastic constants of the unrelaxed B3 calculations before projection to the proper symmetry.

Alloy	SB	$c_{11}$	$c_{22}$	$c_{33}$	$c_{12}$	$c_{13}$	$c_{23}$	$c_{44}$	$c_{55}$	$c_{66}$	$c_{14}$	$c_{15}$	$c_{16}$	$c_{24}$	$c_{25}$	$c_{26}$	$c_{34}$	$c_{35}$	$c_{36}$	$c_{45}$	$c_{46}$	$c_{56}$	
AlN	B3	285	285	285	153	153	153	218	218	218	0	0	0	0	0	0	0	-1	0	0	0	0	0
HfN	B3	292	290	290	150	153	148	143	143	143	0	-1	0	-1	-1	-1	1	-1	0	-1	1	-1	
$\text{Hf}_{0.75}\text{Al}_{0.25}\text{N}$	B3	269	269	270	141	142	143	132	132	132	1	1	1	-1	-1	1	-1	1	-1	1	1	0	
$\text{Hf}_{0.50}\text{Al}_{0.50}\text{N}$	B3	250	250	251	136	138	136	130	130	131	0	2	-1	0	-3	-1	1	2	0	0	1	1	
$\text{Hf}_{0.25}\text{Al}_{0.75}\text{N}$	B3	255	256	256	141	143	143	149	149	150	1	2	1	-1	-2	1	-1	1	-2	1	1	-1	
$\text{Hf}_{0.75}\text{Ti}_{0.25}\text{N}$	B3	283	289	283	150	152	150	141	141	141	1	-3	0	0	-3	0	0	-3	0	-1	0	-1	
$\text{Hf}_{0.50}\text{Ti}_{0.50}\text{N}$	B3	286	285	287	151	155	151	138	139	138	0	1	0	0	0	0	0	1	0	0	0	0	
$\text{Hf}_{0.25}\text{Ti}_{0.75}\text{N}$	B3	287	287	287	154	154	154	138	138	137	1	0	-1	1	-1	-1	1	0	-1	0	0	0	
$\text{Hf}_{0.75}\text{Zr}_{0.25}\text{N}$	B3	286	287	287	152	157	153	140	140	140	1	-1	1	-1	-1	-1	1	-1	1	-1	1	-1	
$\text{Hf}_{0.50}\text{Zr}_{0.50}\text{N}$	B3	270	272	270	145	150	145	134	134	134	1	0	0	-1	0	-1	0	0	1	-1	1	-1	
$\text{Hf}_{0.25}\text{Zr}_{0.75}\text{N}$	B3	260	263	261	140	146	140	129	129	129	1	2	1	0	2	0	1	2	1	-1	1	-1	
TiN	B3	290	286	300	151	156	157	138	139	138	0	4	1	1	3	1	1	4	0	1	0	1	
$\text{Ti}_{0.75}\text{Al}_{0.25}\text{N}$	B3	280	281	280	152	153	153	145	146	144	1	2	1	-1	-1	1	-1	2	-1	1	1	0	
$\text{Ti}_{0.50}\text{Al}_{0.50}\text{N}$	B3	277	276	275	156	158	156	154	156	154	2	-1	0	2	-6	-2	2	-1	-1	0	1	0	
$\text{Ti}_{0.25}\text{Al}_{0.75}\text{N}$	B3	270	272	269	151	152	152	174	174	173	0	2	1	-1	-1	1	-1	2	-1	1	1	-1	
ZrN	B3	257	259	257	143	149	143	125	125	125	1	0	0	0	0	0	0	0	1	-1	1	-1	
$\text{Zr}_{0.75}\text{Al}_{0.25}\text{N}$	B3	245	246	246	140	141	141	118	119	118	1	1	1	-1	-2	1	-1	1	-1	1	1	0	
$\text{Zr}_{0.50}\text{Al}_{0.50}\text{N}$	B3	233	232	234	135	137	135	118	117	118	0	2	0	0	-3	0	0	2	0	0	1	0	
$\text{Zr}_{0.25}\text{Al}_{0.75}\text{N}$	B3	240	241	240	135	137	137	140	140	141	1	1	1	-1	-2	1	0	1	-2	1	1	-1	
$\text{Zr}_{0.75}\text{Ti}_{0.25}\text{N}$	B3	258	257	259	142	147	141	125	125	125	1	0	0	0	0	0	0	0	1	-1	0	-1	
$\text{Zr}_{0.50}\text{Ti}_{0.50}\text{N}$	B3	265	262	265	145	149	145	126	127	126	0	-1	0	0	-1	0	0	0	0	0	0	0	
$\text{Zr}_{0.25}\text{Ti}_{0.75}\text{N}$	B3	277	275	277	151	152	151	131	132	131	0	0	0	0	-1	0	1	-1	0	0	0	0	

Table III: Elastic constants of the unrelaxed B4 calculations before projection to the proper symmetry.

Alloy	SB	$c_{11}$	$c_{22}$	$c_{33}$	$c_{12}$	$c_{13}$	$c_{23}$	$c_{44}$	$c_{55}$	$c_{66}$	$c_{14}$	$c_{15}$	$c_{16}$	$c_{24}$	$c_{25}$	$c_{26}$	$c_{34}$	$c_{35}$	$c_{36}$	$c_{45}$	$c_{46}$	$c_{56}$
AlN	B4	438	440	445	96	61	62	124	124	170	0	0	-1	0	0	-1	0	0	-1	0	0	0
HfN	B4	305	307	270	129	126	130	55	55	88	0	4	0	0	4	0	0	6	3	0	0	0
Hf <sub>0.75</sub> Al <sub>0.25</sub> N	B4	302	300	275	128	119	121	52	52	86	0	0	-1	0	0	0	0	0	0	0	0	0
Hf <sub>0.50</sub> Al <sub>0.50</sub> N	B4	301	299	286	119	105	108	58	55	89	-3	0	-1	3	1	0	0	0	2	-1	0	-2
Hf <sub>0.25</sub> Al <sub>0.75</sub> N	B4	332	328	326	108	86	93	75	77	109	0	-1	-5	0	-1	-6	-1	0	-7	-1	0	1
Hf <sub>0.75</sub> Ti <sub>0.25</sub> N	B4	311	309	289	131	133	134	61	62	89	0	1	-2	0	1	-2	0	1	0	0	0	0
Hf <sub>0.50</sub> Ti <sub>0.50</sub> N	B4	313	310	298	133	132	132	68	68	90	-3	0	0	2	0	0	0	0	1	0	0	-2
Hf <sub>0.25</sub> Ti <sub>0.75</sub> N	B4	308	308	301	130	129	129	73	73	89	0	0	-1	0	0	0	0	0	-1	0	0	0
Hf <sub>0.75</sub> Zr <sub>0.25</sub> N	B4	302	305	271	135	130	134	56	55	84	0	-1	0	0	-1	0	0	-1	1	0	0	0
Hf <sub>0.50</sub> Zr <sub>0.50</sub> N	B4	297	297	271	136	131	133	56	56	80	1	-2	-2	2	-2	-1	2	-2	0	0	0	0
Hf <sub>0.25</sub> Zr <sub>0.75</sub> N	B4	284	282	266	129	127	126	56	56	77	0	0	-1	0	1	0	0	1	-1	0	0	0
TiN	B4	310	310	303	134	134	133	77	77	89	0	0	-1	0	0	1	0	0	0	-1	0	0
Ti <sub>0.75</sub> Al <sub>0.25</sub> N	B4	332	328	328	127	121	124	73	73	100	0	0	-1	0	0	0	0	0	1	0	0	0
Ti <sub>0.50</sub> Al <sub>0.50</sub> N	B4	343	345	346	118	106	105	79	77	113	0	-1	-2	-1	0	-1	0	1	1	0	0	1
Ti <sub>0.25</sub> Al <sub>0.75</sub> N	B4	374	369	377	105	83	85	93	94	132	1	-1	-2	0	0	-1	0	0	-1	0	0	0
ZrN	B4	278	279	258	130	123	122	58	58	75	0	2	0	0	2	1	0	2	-1	0	0	0
Zr <sub>0.75</sub> Al <sub>0.25</sub> N	B4	272	271	262	121	115	117	50	50	75	0	0	-1	-1	0	1	-1	0	0	-1	0	0
Zr <sub>0.50</sub> Al <sub>0.50</sub> N	B4	276	274	270	114	102	104	53	50	79	-3	0	-2	3	1	0	1	-1	1	-1	0	-3
Zr <sub>0.25</sub> Al <sub>0.75</sub> N	B4	314	308	311	105	84	90	70	71	102	0	-1	0	0	0	1	-2	1	-1	-1	0	1
Zr <sub>0.75</sub> Ti <sub>0.25</sub> N	B4	282	284	268	128	122	121	62	62	78	0	0	-1	0	0	1	0	0	-1	0	0	0
Zr <sub>0.50</sub> Ti <sub>0.50</sub> N	B4	286	287	274	128	123	122	66	66	79	-2	-1	0	3	-1	1	0	0	-1	0	0	-2
Zr <sub>0.25</sub> Ti <sub>0.75</sub> N	B4	291	292	287	127	126	125	71	71	82	0	-1	0	0	-1	2	1	0	0	0	0	0

## B. Relaxed calculations

Table IV: Elastic constants of the relaxed B1 calculations before projection to the proper symmetry.

Alloy	SB	$c_{11}$	$c_{22}$	$c_{33}$	$c_{12}$	$c_{13}$	$c_{23}$	$c_{44}$	$c_{55}$	$c_{66}$	$c_{14}$	$c_{15}$	$c_{16}$	$c_{24}$	$c_{25}$	$c_{26}$	$c_{34}$	$c_{35}$	$c_{36}$	$c_{45}$	$c_{46}$	$c_{56}$
AlN	B1	431	429	435	166	169	168	307	307	307	0	0	0	0	0	0	0	0	0	0	0	0
HfN	B1	594	607	594	108	119	108	127	131	127	-4	-1	3	1	3	1	3	-1	-4	-1	1	-1
Hf <sub>0.75</sub> Al <sub>0.25</sub> N	B1	523	521	529	126	121	126	148	151	142	2	1	0	-1	-2	0	0	2	0	3	6	-3
Hf <sub>0.50</sub> Al <sub>0.50</sub> N	B1	464	445	471	145	138	144	171	182	170	-5	0	1	3	2	-3	1	1	3	0	11	2
Hf <sub>0.25</sub> Al <sub>0.75</sub> N	B1	424	429	434	158	158	156	220	222	220	0	0	2	-2	1	1	0	1	1	4	4	-3
Hf <sub>0.75</sub> Ti <sub>0.25</sub> N	B1	578	584	580	110	118	111	134	136	133	-1	1	1	0	-1	1	0	0	-2	1	0	-1
Hf <sub>0.50</sub> Ti <sub>0.50</sub> N	B1	572	556	575	117	121	118	140	145	140	-2	1	2	4	-1	-3	-1	1	-1	1	1	0
Hf <sub>0.25</sub> Ti <sub>0.75</sub> N	B1	577	573	580	118	128	120	153	156	151	0	1	0	1	-1	1	1	0	-2	1	-1	0
Hf <sub>0.75</sub> Zr <sub>0.25</sub> N	B1	580	591	580	106	116	106	127	131	127	-2	0	3	0	1	1	2	-1	-3	-1	0	-1
Hf <sub>0.50</sub> Zr <sub>0.50</sub> N	B1	565	575	566	106	116	104	127	130	127	-2	-1	2	0	0	1	2	0	-2	-1	0	-1
Hf <sub>0.25</sub> Zr <sub>0.75</sub> N	B1	551	561	551	103	113	104	126	128	126	-2	1	2	0	1	1	1	0	-2	-1	0	-1
TiN	B1	579	587	585	134	141	132	166	165	166	1	2	0	2	-8	2	0	2	2	2	-3	2
Ti <sub>0.75</sub> Al <sub>0.25</sub> N	B1	534	529	540	140	136	141	182	183	178	1	0	0	-1	0	-1	1	0	1	1	1	0
Ti <sub>0.50</sub> Al <sub>0.50</sub> N	B1	502	470	504	158	150	159	212	221	209	-2	0	-1	2	0	-3	-1	-1	5	0	2	0
Ti <sub>0.25</sub> Al <sub>0.75</sub> N	B1	435	444	450	162	159	162	250	250	248	2	0	0	0	-1	1	0	0	-2	0	-1	0
ZrN	B1	541	549	541	108	116	108	125	126	125	-1	-1	1	1	0	1	1	-1	-1	0	-1	
Zr <sub>0.75</sub> Al <sub>0.25</sub> N	B1	476	474	482	126	121	125	140	142	134	1	0	-1	0	-2	0	1	1	0	2	5	-1
Zr <sub>0.50</sub> Al <sub>0.50</sub> N	B1	432	411	437	143	137	143	163	174	161	-4	-1	1	3	2	-4	1	0	2	0	10	2
Zr <sub>0.25</sub> Al <sub>0.75</sub> N	B1	408	411	415	158	157	155	214	216	215	0	-1	0	-1	1	0	1	0	0	3	3	-2
Zr <sub>0.75</sub> Ti <sub>0.25</sub> N	B1	537	541	538	107	117	108	130	131	129	-1	0	0	1	-1	0	1	0	-2	0	0	-1
Zr <sub>0.50</sub> Ti <sub>0.50</sub> N	B1	542	537	542	115	120	113	136	141	137	-1	1	3	3	-1	-2	-1	1	-1	1	0	0
Zr <sub>0.25</sub> Ti <sub>0.75</sub> N	B1	568	567	570	119	128	120	150	153	149	0	1	-1	0	-1	-1	1	0	-1	1	-1	0

Table V: Elastic constants of the relaxed B3 calculations before projection to the proper symmetry.

Alloy	SB	$c_{11}$	$c_{22}$	$c_{33}$	$c_{12}$	$c_{13}$	$c_{23}$	$c_{44}$	$c_{55}$	$c_{66}$	$c_{14}$	$c_{15}$	$c_{16}$	$c_{24}$	$c_{25}$	$c_{26}$	$c_{34}$	$c_{35}$	$c_{36}$	$c_{45}$	$c_{46}$	$c_{56}$
AlN	B3	285	285	285	152	152	152	178	178	178	0	0	0	0	0	0	0	0	0	0	0	0
HfN	B3	292	293	291	151	154	151	93	94	93	0	0	0	0	-1	0	1	0	0	0	0	0
Hf <sub>0.75</sub> Al <sub>0.25</sub> N	B3	274	275	274	144	144	144	100	101	99	2	2	1	-1	-4	1	-1	2	-3	2	2	-1
Hf <sub>0.50</sub> Al <sub>0.50</sub> N	B3	260	261	263	144	145	143	104	109	104	-1	2	0	-1	-5	0	-1	1	1	-1	8	1
Hf <sub>0.25</sub> Al <sub>0.75</sub> N	B3	262	262	265	144	143	143	127	127	126	3	0	0	0	-2	0	1	0	-3	2	7	-1
Hf <sub>0.75</sub> Ti <sub>0.25</sub> N	B3	286	288	287	149	153	148	92	94	92	0	1	-1	1	-2	0	0	1	0	0	0	0
Hf <sub>0.50</sub> Ti <sub>0.50</sub> N	B3	286	285	287	149	152	149	92	93	92	-1	1	0	0	-2	1	-1	1	0	0	0	0
Hf <sub>0.25</sub> Ti <sub>0.75</sub> N	B3	289	288	290	152	153	152	92	92	92	0	0	-1	1	-2	0	0	0	-1	0	0	0
Hf <sub>0.75</sub> Zr <sub>0.25</sub> N	B3	280	282	280	147	151	147	91	92	91	0	0	0	0	-2	0	0	0	0	0	0	0
Hf <sub>0.50</sub> Zr <sub>0.50</sub> N	B3	272	273	271	145	151	145	89	91	89	0	1	0	0	-2	0	0	1	0	0	0	0
Hf <sub>0.25</sub> Zr <sub>0.75</sub> N	B3	263	265	263	142	148	142	88	89	88	0	0	0	0	-1	0	0	0	0	0	0	0
TiN	B3	293	292	294	156	153	156	90	92	90	0	0	0	0	-2	1	0	0	0	0	0	0
Ti <sub>0.75</sub> Al <sub>0.25</sub> N	B3	282	283	282	154	154	154	104	104	102	2	2	1	-1	-3	1	-1	2	-3	0	0	0
Ti <sub>0.50</sub> Al <sub>0.50</sub> N	B3	274	275	273	153	155	154	115	118	114	0	2	1	0	-4	0	0	2	0	0	2	0
Ti <sub>0.25</sub> Al <sub>0.75</sub> N	B3	272	270	271	151	153	153	139	138	137	2	1	1	0	-2	1	0	1	-2	1	2	-1
ZrN	B3	258	259	257	142	149	142	86	87	86	0	0	-1	0	-1	0	0	0	0	0	0	0
Zr <sub>0.75</sub> Al <sub>0.25</sub> N	B3	247	247	246	141	141	140	92	93	91	3	1	1	-1	-5	1	-1	2	-4	1	2	-1
Zr <sub>0.50</sub> Al <sub>0.50</sub> N	B3	238	240	242	143	142	142	97	101	96	-1	1	0	0	-6	0	0	0	1	-1	8	0
Zr <sub>0.25</sub> Al <sub>0.75</sub> N	B3	254	250	256	146	145	146	123	122	123	4	-1	-1	0	-4	-1	1	-1	-4	2	6	-1
Zr <sub>0.75</sub> Ti <sub>0.25</sub> N	B3	261	262	262	144	147	143	86	87	86	0	0	-1	1	-3	0	0	0	0	0	0	0
Zr <sub>0.50</sub> Ti <sub>0.50</sub> N	B3	270	269	269	147	148	148	88	88	87	-1	0	0	1	-2	1	-1	1	0	0	1	0
Zr <sub>0.25</sub> Ti <sub>0.75</sub> N	B3	283	281	284	154	154	154	89	89	89	0	0	-1	1	-2	0	0	0	-1	0	1	0

Table VI: Elastic constants of the relaxed B4 calculations before projection to the proper symmetry.

Alloy	SB	$c_{11}$	$c_{22}$	$c_{33}$	$c_{12}$	$c_{13}$	$c_{23}$	$c_{44}$	$c_{55}$	$c_{66}$	$c_{14}$	$c_{15}$	$c_{16}$	$c_{24}$	$c_{25}$	$c_{26}$	$c_{34}$	$c_{35}$	$c_{36}$	$c_{45}$	$c_{46}$	$c_{56}$
AlN	B4	376	375	352	128	98	98	112	112	123	0	0	0	0	0	0	0	0	0	0	0	0
HfN	B4	251	252	220	162	162	161	47	47	47	0	0	0	0	0	1	0	0	0	1	0	0
$Hf_{0.75}Al_{0.25}N$	$B4 \rightarrow B_k$	295	296	359	205	109	117	104	110	47	-1	2	-3	-1	-1	3	0	1	0	0	-1	1
$Hf_{0.50}Al_{0.50}N$	$B4 \rightarrow B_k$	295	302	110	175	150	141	107	111	60	6	-7	6	-1	-5	4	-12	11	-1	-1	0	3
$Hf_{0.25}Al_{0.75}N$	B4	310	295	216	142	125	123	76	97	85	-1	0	5	2	-1	-4	-4	-5	4	3	-5	0
$Hf_{0.75}Ti_{0.25}N$	$B4 \rightarrow B_k$	297	296	493	212	107	104	113	114	45	0	0	-1	0	0	5	0	0	-3	0	0	0
$Hf_{0.50}Ti_{0.50}N$	$B4 \rightarrow B_k$	301	304	491	211	105	102	120	120	49	0	0	0	0	0	4	0	-1	-2	0	0	0
$Hf_{0.25}Ti_{0.75}N$	$B4 \rightarrow B_k$	309	311	500	213	107	105	128	129	50	0	0	0	0	0	5	0	0	-2	0	0	0
$Hf_{0.75}Zr_{0.25}N$	$B4 \rightarrow B_k$	286	292	495	213	106	103	106	107	43	0	0	-1	0	0	7	0	0	-3	-1	0	0
$Hf_{0.50}Zr_{0.50}N$	$B4 \rightarrow B_k$	283	290	483	207	104	101	107	107	43	0	0	-1	0	0	6	0	0	-2	-1	0	0
$Hf_{0.25}Zr_{0.75}N$	$B4 \rightarrow B_k$	282	289	470	201	103	100	106	107	43	0	0	0	0	0	6	0	0	-2	0	0	0
TiN	$B4 \rightarrow B_k$	316	325	524	220	112	109	139	138	53	0	0	0	0	0	7	0	0	-3	0	0	0
$Ti_{0.75}Al_{0.25}N$	$B4 \rightarrow B_k$	309	310	438	214	119	120	138	138	51	0	0	1	0	0	1	0	0	1	-1	0	0
$Ti_{0.50}Al_{0.50}N$	$B4 \rightarrow B_k$	315	313	363	197	127	129	148	147	59	0	0	1	-1	0	0	0	-1	2	2	0	1
$Ti_{0.25}Al_{0.75}N$	B4	319	310	214	136	134	138	87	89	91	6	0	2	0	-2	1	-10	1	-1	0	-1	2
ZrN	$B4 \rightarrow B_k$	279	290	458	195	103	99	107	106	44	0	0	2	0	0	6	0	0	-2	1	0	0
$Zr_{0.75}Al_{0.25}N$	$B4 \rightarrow B_k$	276	276	320	196	107	110	99	103	42	0	1	-2	0	-2	2	0	2	0	-2	-1	1
$Zr_{0.50}Al_{0.50}N$	$B4 \rightarrow B_k$	289	284	202	178	128	123	111	110	55	-1	-1	4	-1	0	2	-1	-2	1	0	-1	1
$Zr_{0.25}Al_{0.75}N$	B4	306	298	190	147	116	129	82	95	78	-1	-2	1	-1	-4	-2	-1	3	6	4	-2	0
$Zr_{0.75}Ti_{0.25}N$	$B4 \rightarrow B_k$	287	288	453	201	101	100	110	111	44	0	0	0	0	0	4	0	0	-2	0	0	0
$Zr_{0.50}Ti_{0.50}N$	$B4 \rightarrow B_k$	295	297	461	205	103	101	116	117	47	0	0	0	0	0	4	0	-1	-1	-1	0	0
$Zr_{0.25}Ti_{0.75}N$	$B4 \rightarrow B_k$	305	308	485	211	106	105	124	126	49	0	0	0	0	0	4	0	0	-2	0	0	0

## II. SQS COORDINATES

B1 A<sub>0.25</sub>B<sub>0.75</sub>N POSCAR

```

B36 A12 N48
4.18
2.00000000 2.00000000 0.00000000
0.00000000 2.00000000 2.00000000
1.50000000 0.00000000 1.50000000
A B N
12 36 48
direct
0.75000000 0.00000000 0.66666667 A
0.00000000 0.50000000 0.00000000 A
0.25000000 0.75000000 1.00000000 A
0.50000000 0.25000000 0.00000000 A
0.50000000 0.75000000 1.00000000 A
0.00000000 0.50000000 0.33333333 A
0.25000000 0.75000000 0.33333333 A
0.25000000 0.75000000 0.66666667 A
0.50000000 0.75000000 0.66666667 A
0.75000000 0.50000000 0.33333333 A
0.75000000 0.75000000 0.33333333 A
0.75000000 0.75000000 0.66666667 A
0.00000000 0.00000000 0.00000000 B
0.25000000 0.00000000 0.00000000 B
0.50000000 0.00000000 0.00000000 B
0.75000000 0.00000000 0.00000000 B
0.00000000 0.00000000 0.33333333 B
0.00000000 0.00000000 0.66666667 B
0.25000000 0.00000000 0.33333333 B
0.25000000 0.00000000 0.66666667 B
0.50000000 0.00000000 0.33333333 B
0.50000000 0.00000000 0.66666667 B
0.75000000 0.00000000 0.33333333 B
0.00000000 0.25000000 0.00000000 B
0.00000000 0.75000000 1.00000000 B
0.25000000 0.25000000 0.00000000 B
0.25000000 0.50000000 0.00000000 B
0.50000000 0.50000000 0.00000000 B
0.75000000 0.25000000 0.00000000 B
0.75000000 0.50000000 0.00000000 B
0.75000000 0.75000000 0.00000000 B
0.00000000 0.25000000 0.33333333 B
0.00000000 0.75000000 0.33333333 B
0.00000000 0.25000000 0.66666667 B
0.00000000 0.50000000 0.66666667 B
0.00000000 0.75000000 0.66666667 B
0.25000000 0.25000000 0.33333333 B
0.25000000 0.50000000 0.33333333 B
0.25000000 0.25000000 0.66666667 B
0.25000000 0.50000000 0.66666667 B
0.50000000 0.25000000 0.33333333 B
0.50000000 0.50000000 0.33333333 B
0.50000000 0.75000000 0.33333333 B
0.50000000 0.25000000 0.66666667 B
0.50000000 0.50000000 0.66666667 B
0.50000000 0.75000000 0.66666667 B
0.75000000 0.25000000 0.33333333 B

```

0.75000000 0.25000000 0.66666667 B  
0.75000000 0.50000000 0.66666667 B  
0.12500000 0.12500000 0.16666667 N  
0.37500000 0.12500000 0.16666667 N  
0.62500000 0.12500000 0.16666667 N  
0.87500000 0.12500000 0.16666667 N  
0.12500000 0.12500000 0.50000000 N  
0.12500000 0.12500000 0.83333333 N  
0.37500000 0.12500000 0.50000000 N  
0.37500000 0.12500000 0.83333333 N  
0.62500000 0.12500000 0.50000000 N  
0.62500000 0.12500000 0.83333333 N  
0.87500000 0.12500000 0.50000000 N  
0.87500000 0.12500000 0.83333333 N  
0.12500000 0.37500000 0.16666667 N  
0.12500000 0.62500000 0.16666667 N  
0.12500000 0.87500000 0.16666667 N  
0.37500000 0.37500000 0.16666667 N  
0.37500000 0.62500000 0.16666667 N  
0.37500000 0.87500000 0.16666667 N  
0.62500000 0.37500000 0.16666667 N  
0.62500000 0.62500000 0.16666667 N  
0.62500000 0.87500000 0.16666667 N  
0.87500000 0.37500000 0.16666667 N  
0.87500000 0.62500000 0.16666667 N  
0.87500000 0.87500000 0.16666667 N  
0.12500000 0.37500000 0.50000000 N  
0.12500000 0.62500000 0.50000000 N  
0.12500000 0.87500000 0.50000000 N  
0.12500000 0.37500000 0.83333333 N  
0.12500000 0.62500000 0.83333333 N  
0.12500000 0.87500000 0.83333333 N  
0.37500000 0.37500000 0.50000000 N  
0.37500000 0.62500000 0.50000000 N  
0.37500000 0.87500000 0.50000000 N  
0.37500000 0.37500000 0.83333333 N  
0.37500000 0.62500000 0.83333333 N  
0.37500000 0.87500000 0.83333333 N  
0.62500000 0.37500000 0.50000000 N  
0.62500000 0.62500000 0.50000000 N  
0.62500000 0.87500000 0.50000000 N  
0.62500000 0.37500000 0.83333333 N  
0.62500000 0.62500000 0.83333333 N  
0.62500000 0.87500000 0.83333333 N  
0.87500000 0.37500000 0.50000000 N  
0.87500000 0.62500000 0.50000000 N  
0.87500000 0.87500000 0.50000000 N  
0.87500000 0.37500000 0.83333333 N  
0.87500000 0.62500000 0.83333333 N  
0.87500000 0.87500000 0.83333333 N

B1 A<sub>0.50</sub>B<sub>0.50</sub>N POSCAR

A0.5B0.5N  
 4.18  
 2.00000000 2.00000000 0.00000000  
 0.00000000 2.00000000 2.00000000  
 1.50000000 0.00000000 1.50000000  
 N B A  
 48 24 24  
 D  
 0.12500000 0.12500000 0.83333333  
 0.12500000 0.37500000 0.83333333  
 0.12500000 0.62500000 0.83333333  
 0.12500000 0.87500000 0.83333333  
 0.12500000 0.12500000 0.16666667  
 0.12500000 0.12500000 0.50000000  
 0.12500000 0.37500000 0.16666667  
 0.12500000 0.37500000 0.50000000  
 0.12500000 0.62500000 0.16666667  
 0.12500000 0.87500000 0.16666667  
 0.12500000 0.62500000 0.50000000  
 0.12500000 0.87500000 0.50000000  
 0.37500000 0.12500000 0.16666667  
 0.37500000 0.12500000 0.50000000  
 0.37500000 0.12500000 0.83333333  
 0.37500000 0.37500000 0.50000000  
 0.37500000 0.37500000 0.83333333  
 0.37500000 0.62500000 0.16666667  
 0.37500000 0.62500000 0.50000000  
 0.37500000 0.62500000 0.83333333  
 0.37500000 0.87500000 0.16666667  
 0.37500000 0.87500000 0.50000000  
 0.37500000 0.87500000 0.83333333  
 0.37500000 0.37500000 0.16666667  
 0.62500000 0.37500000 0.83333333  
 0.62500000 0.12500000 0.50000000  
 0.62500000 0.12500000 0.83333333  
 0.62500000 0.12500000 0.16666667  
 0.62500000 0.37500000 0.16666667  
 0.62500000 0.37500000 0.50000000  
 0.62500000 0.62500000 0.83333333  
 0.62500000 0.87500000 0.16666667  
 0.62500000 0.87500000 0.83333333  
 0.62500000 0.62500000 0.16666667  
 0.62500000 0.87500000 0.50000000  
 0.87500000 0.12500000 0.16666667  
 0.87500000 0.12500000 0.50000000  
 0.87500000 0.37500000 0.16666667  
 0.87500000 0.37500000 0.50000000  
 0.87500000 0.37500000 0.83333333  
 0.87500000 0.62500000 0.16666667  
 0.87500000 0.62500000 0.83333333  
 0.87500000 0.87500000 0.16666667  
 0.87500000 0.87500000 0.83333333  
 0.87500000 0.12500000 0.83333333  
 0.87500000 0.62500000 0.50000000  
 0.87500000 0.87500000 0.50000000  
 0.00000000 0.00000000 0.00000000

0.00000000 0.75000000 0.00000000  
0.00000000 0.75000000 0.33333333  
0.00000000 1.00000000 0.33333333  
0.00000000 0.50000000 0.66666667  
0.00000000 0.75000000 0.66666667  
0.00000000 1.00000000 0.66666667  
0.25000000 0.00000000 0.33333333  
0.25000000 0.00000000 0.00000000  
0.25000000 0.25000000 0.00000000  
0.25000000 0.25000000 0.33333333  
0.25000000 0.25000000 0.66666667  
0.25000000 0.50000000 0.66666667  
0.25000000 1.00000000 0.66666667  
0.50000000 0.00000000 0.66666667  
0.50000000 0.25000000 0.33333333  
0.50000000 0.75000000 0.00000000  
0.50000000 0.75000000 0.66666667  
0.50000000 1.00000000 0.33333333  
0.50000000 0.75000000 0.33333333  
0.75000000 0.00000000 0.00000000  
0.75000000 0.25000000 0.66666667  
0.75000000 0.25000000 0.00000000  
0.75000000 0.25000000 0.33333333  
0.00000000 0.25000000 0.00000000  
0.00000000 0.50000000 0.00000000  
0.00000000 0.25000000 0.33333333  
0.00000000 0.50000000 0.33333333  
0.00000000 0.25000000 0.66666667  
0.25000000 0.50000000 0.00000000  
0.25000000 0.75000000 0.00000000  
0.25000000 0.75000000 0.33333333  
0.25000000 0.75000000 0.66666667  
0.25000000 0.50000000 0.33333333  
0.50000000 0.25000000 0.66666667  
0.50000000 0.00000000 0.00000000  
0.50000000 0.25000000 0.00000000  
0.50000000 0.50000000 0.00000000  
0.50000000 0.50000000 0.66666667  
0.50000000 0.50000000 0.33333333  
0.75000000 0.50000000 0.00000000  
0.75000000 0.50000000 0.33333333  
0.75000000 0.50000000 0.66666667  
0.75000000 0.75000000 0.00000000  
0.75000000 0.75000000 0.33333333  
0.75000000 0.75000000 0.66666667  
0.75000000 1.00000000 0.66666667  
0.75000000 1.00000000 0.33333333

B1 A<sub>0.75</sub>B<sub>0.25</sub>N POSCAR

A36 B12 N48

4.18

2.00000000 2.00000000 0.00000000  
 0.00000000 2.00000000 2.00000000  
 1.50000000 0.00000000 1.50000000

B A N

12 36 48

direct

0.75000000 0.00000000 0.66666667 B  
 0.00000000 0.50000000 0.00000000 B  
 0.25000000 0.75000000 1.00000000 B  
 0.50000000 0.25000000 0.00000000 B  
 0.50000000 0.75000000 1.00000000 B  
 0.00000000 0.50000000 0.33333333 B  
 0.25000000 0.75000000 0.33333333 B  
 0.25000000 0.75000000 0.66666667 B  
 0.50000000 0.75000000 0.66666667 B  
 0.75000000 0.50000000 0.33333333 B  
 0.75000000 0.75000000 0.33333333 B  
 0.75000000 0.75000000 0.66666667 B  
 0.00000000 0.00000000 0.00000000 A  
 0.25000000 0.00000000 0.00000000 A  
 0.50000000 0.00000000 0.00000000 A  
 0.75000000 0.00000000 0.00000000 A  
 0.00000000 0.00000000 0.33333333 A  
 0.00000000 0.00000000 0.66666667 A  
 0.25000000 0.00000000 0.33333333 A  
 0.25000000 0.00000000 0.66666667 A  
 0.50000000 0.00000000 0.33333333 A  
 0.50000000 0.00000000 0.66666667 A  
 0.75000000 0.00000000 0.33333333 A  
 0.00000000 0.25000000 0.00000000 A  
 0.00000000 0.75000000 1.00000000 A  
 0.25000000 0.25000000 0.00000000 A  
 0.25000000 0.50000000 0.00000000 A  
 0.50000000 0.50000000 0.00000000 A  
 0.75000000 0.25000000 0.00000000 A  
 0.75000000 0.50000000 0.00000000 A  
 0.75000000 0.75000000 0.00000000 A  
 0.00000000 0.25000000 0.33333333 A  
 0.00000000 0.75000000 0.33333333 A  
 0.00000000 0.25000000 0.66666667 A  
 0.00000000 0.50000000 0.66666667 A  
 0.00000000 0.75000000 0.66666667 A  
 0.25000000 0.25000000 0.33333333 A  
 0.25000000 0.50000000 0.33333333 A  
 0.25000000 0.25000000 0.66666667 A  
 0.25000000 0.50000000 0.66666667 A  
 0.50000000 0.25000000 0.33333333 A  
 0.50000000 0.50000000 0.33333333 A  
 0.50000000 0.75000000 0.33333333 A  
 0.50000000 0.25000000 0.66666667 A  
 0.50000000 0.50000000 0.66666667 A  
 0.75000000 0.25000000 0.33333333 A  
 0.75000000 0.25000000 0.66666667 A  
 0.75000000 0.50000000 0.66666667 A  
 0.12500000 0.12500000 0.16666667 N

0.37500000 0.12500000 0.16666667 N  
0.62500000 0.12500000 0.16666667 N  
0.87500000 0.12500000 0.16666667 N  
0.12500000 0.12500000 0.50000000 N  
0.12500000 0.12500000 0.83333333 N  
0.37500000 0.12500000 0.50000000 N  
0.37500000 0.12500000 0.83333333 N  
0.62500000 0.12500000 0.50000000 N  
0.62500000 0.12500000 0.83333333 N  
0.87500000 0.12500000 0.50000000 N  
0.87500000 0.12500000 0.83333333 N  
0.12500000 0.37500000 0.16666667 N  
0.12500000 0.62500000 0.16666667 N  
0.12500000 0.87500000 0.16666667 N  
0.37500000 0.37500000 0.16666667 N  
0.37500000 0.62500000 0.16666667 N  
0.37500000 0.87500000 0.16666667 N  
0.62500000 0.37500000 0.16666667 N  
0.62500000 0.62500000 0.16666667 N  
0.62500000 0.87500000 0.16666667 N  
0.87500000 0.37500000 0.16666667 N  
0.87500000 0.62500000 0.16666667 N  
0.87500000 0.87500000 0.16666667 N  
0.12500000 0.37500000 0.50000000 N  
0.12500000 0.62500000 0.50000000 N  
0.12500000 0.87500000 0.50000000 N  
0.37500000 0.37500000 0.50000000 N  
0.37500000 0.62500000 0.50000000 N  
0.37500000 0.87500000 0.50000000 N  
0.37500000 0.37500000 0.83333333 N  
0.37500000 0.62500000 0.83333333 N  
0.37500000 0.87500000 0.83333333 N  
0.62500000 0.37500000 0.50000000 N  
0.62500000 0.62500000 0.50000000 N  
0.62500000 0.87500000 0.50000000 N  
0.62500000 0.37500000 0.83333333 N  
0.62500000 0.62500000 0.83333333 N  
0.62500000 0.87500000 0.83333333 N  
0.87500000 0.37500000 0.50000000 N  
0.87500000 0.62500000 0.50000000 N  
0.87500000 0.87500000 0.50000000 N  
0.87500000 0.37500000 0.83333333 N  
0.87500000 0.62500000 0.83333333 N  
0.87500000 0.87500000 0.83333333 N

B3 A<sub>0.25</sub>B<sub>0.75</sub>N POSCAR

B36 A12 N48

4.18

2.00000000 2.00000000 0.00000000  
 0.00000000 2.00000000 2.00000000  
 1.50000000 0.00000000 1.50000000

A B N

12 36 48

direct

0.75000000 0.00000000 0.66666667 A  
 0.00000000 0.50000000 0.00000000 A  
 0.25000000 0.75000000 1.00000000 A  
 0.50000000 0.25000000 0.00000000 A  
 0.50000000 0.75000000 1.00000000 A  
 0.00000000 0.50000000 0.33333333 A  
 0.25000000 0.75000000 0.33333333 A  
 0.25000000 0.75000000 0.66666667 A  
 0.50000000 0.75000000 0.66666667 A  
 0.75000000 0.50000000 0.33333333 A  
 0.75000000 0.75000000 0.33333333 A  
 0.75000000 0.75000000 0.66666667 A  
 0.00000000 0.00000000 0.00000000 B  
 0.25000000 0.00000000 0.00000000 B  
 0.50000000 0.00000000 0.00000000 B  
 0.75000000 0.00000000 0.00000000 B  
 0.00000000 0.00000000 0.33333333 B  
 0.00000000 0.00000000 0.66666667 B  
 0.25000000 0.00000000 0.33333333 B  
 0.25000000 0.00000000 0.66666667 B  
 0.50000000 0.00000000 0.33333333 B  
 0.50000000 0.00000000 0.66666667 B  
 0.75000000 0.00000000 0.33333333 B  
 0.00000000 0.25000000 0.00000000 B  
 0.00000000 0.75000000 1.00000000 B  
 0.25000000 0.25000000 0.00000000 B  
 0.25000000 0.50000000 0.00000000 B  
 0.50000000 0.50000000 0.00000000 B  
 0.75000000 0.25000000 0.00000000 B  
 0.75000000 0.50000000 0.00000000 B  
 0.75000000 0.75000000 0.00000000 B  
 0.00000000 0.25000000 0.33333333 B  
 0.00000000 0.75000000 0.33333333 B  
 0.00000000 0.25000000 0.66666667 B  
 0.00000000 0.50000000 0.66666667 B  
 0.00000000 0.75000000 0.66666667 B  
 0.25000000 0.25000000 0.33333333 B  
 0.25000000 0.50000000 0.33333333 B  
 0.25000000 0.25000000 0.66666667 B  
 0.25000000 0.50000000 0.66666667 B  
 0.50000000 0.25000000 0.33333333 B  
 0.50000000 0.50000000 0.33333333 B  
 0.50000000 0.75000000 0.33333333 B  
 0.50000000 0.25000000 0.66666667 B  
 0.50000000 0.50000000 0.66666667 B  
 0.75000000 0.25000000 0.33333333 B  
 0.75000000 0.25000000 0.66666667 B  
 0.75000000 0.50000000 0.66666667 B  
 0.06250000 0.06250000 0.08333334 N

0.31250000 0.06250000 0.08333334 N  
0.56250000 0.06250000 0.08333334 N  
0.81250000 0.06250000 0.08333334 N  
0.06250000 0.06250000 0.41666667 N  
0.06250000 0.06250000 0.75000000 N  
0.31250000 0.06250000 0.41666667 N  
0.31250000 0.06250000 0.75000000 N  
0.56250000 0.06250000 0.41666667 N  
0.56250000 0.06250000 0.75000000 N  
0.81250000 0.06250000 0.41666667 N  
0.81250000 0.06250000 0.75000000 N  
0.06250000 0.31250000 0.08333334 N  
0.06250000 0.56250000 0.08333334 N  
0.06250000 0.81250000 0.08333334 N  
0.31250000 0.31250000 0.08333334 N  
0.31250000 0.56250000 0.08333334 N  
0.31250000 0.81250000 0.08333334 N  
0.56250000 0.31250000 0.08333334 N  
0.56250000 0.56250000 0.08333334 N  
0.56250000 0.81250000 0.08333334 N  
0.81250000 0.31250000 0.08333334 N  
0.81250000 0.56250000 0.08333334 N  
0.81250000 0.81250000 0.08333334 N  
0.06250000 0.31250000 0.41666667 N  
0.06250000 0.56250000 0.41666667 N  
0.06250000 0.81250000 0.41666667 N  
0.06250000 0.31250000 0.75000000 N  
0.06250000 0.56250000 0.75000000 N  
0.06250000 0.81250000 0.75000000 N  
0.31250000 0.31250000 0.41666667 N  
0.31250000 0.56250000 0.41666667 N  
0.31250000 0.81250000 0.41666667 N  
0.31250000 0.31250000 0.75000000 N  
0.31250000 0.56250000 0.75000000 N  
0.31250000 0.81250000 0.75000000 N  
0.56250000 0.31250000 0.41666667 N  
0.56250000 0.56250000 0.41666667 N  
0.56250000 0.81250000 0.41666667 N  
0.56250000 0.31250000 0.75000000 N  
0.56250000 0.56250000 0.75000000 N  
0.56250000 0.81250000 0.75000000 N  
0.81250000 0.31250000 0.41666667 N  
0.81250000 0.56250000 0.41666667 N  
0.81250000 0.81250000 0.41666667 N  
0.81250000 0.31250000 0.75000000 N  
0.81250000 0.56250000 0.75000000 N  
0.81250000 0.81250000 0.75000000 N

B3 A<sub>0.50</sub>B<sub>0.50</sub>N POSCAR

A0.5B0.5N  
 4.18  
 2.00000000 2.00000000 0.00000000  
 0.00000000 2.00000000 2.00000000  
 1.50000000 0.00000000 1.50000000  
 N B A  
 48 24 24  
 D  
 0.06250000 0.06250000 0.75000000  
 0.06250000 0.31250000 0.75000000  
 0.06250000 0.56250000 0.75000000  
 0.06250000 0.81250000 0.75000000  
 0.06250000 0.06250000 0.08333334  
 0.06250000 0.06250000 0.41666667  
 0.06250000 0.31250000 0.08333334  
 0.06250000 0.31250000 0.41666667  
 0.06250000 0.56250000 0.08333334  
 0.06250000 0.81250000 0.08333334  
 0.06250000 0.56250000 0.41666667  
 0.06250000 0.81250000 0.41666667  
 0.31250000 0.06250000 0.08333334  
 0.31250000 0.06250000 0.41666667  
 0.31250000 0.06250000 0.75000000  
 0.31250000 0.31250000 0.41666667  
 0.31250000 0.31250000 0.75000000  
 0.31250000 0.56250000 0.08333334  
 0.31250000 0.56250000 0.41666667  
 0.31250000 0.56250000 0.75000000  
 0.31250000 0.81250000 0.08333334  
 0.31250000 0.81250000 0.41666667  
 0.31250000 0.81250000 0.75000000  
 0.31250000 0.31250000 0.08333334  
 0.56250000 0.31250000 0.75000000  
 0.56250000 0.06250000 0.41666667  
 0.56250000 0.06250000 0.75000000  
 0.56250000 0.06250000 0.08333334  
 0.56250000 0.31250000 0.08333334  
 0.56250000 0.31250000 0.41666667  
 0.56250000 0.56250000 0.75000000  
 0.56250000 0.81250000 0.08333334  
 0.56250000 0.81250000 0.75000000  
 0.56250000 0.56250000 0.08333334  
 0.56250000 0.56250000 0.41666667  
 0.56250000 0.81250000 0.41666667  
 0.81250000 0.06250000 0.08333334  
 0.81250000 0.06250000 0.41666667  
 0.81250000 0.31250000 0.08333334  
 0.81250000 0.31250000 0.41666667  
 0.81250000 0.31250000 0.75000000  
 0.81250000 0.56250000 0.08333334  
 0.81250000 0.56250000 0.75000000  
 0.81250000 0.81250000 0.08333334  
 0.81250000 0.81250000 0.75000000  
 0.81250000 0.06250000 0.75000000  
 0.81250000 0.56250000 0.41666667  
 0.81250000 0.81250000 0.41666667  
 0.00000000 0.00000000 0.00000000

0.00000000 0.75000000 0.00000000  
0.00000000 0.75000000 0.33333333  
0.00000000 1.00000000 0.33333333  
0.00000000 0.50000000 0.66666667  
0.00000000 0.75000000 0.66666667  
0.00000000 1.00000000 0.66666667  
0.25000000 0.00000000 0.33333333  
0.25000000 0.00000000 0.00000000  
0.25000000 0.25000000 0.00000000  
0.25000000 0.25000000 0.33333333  
0.25000000 0.25000000 0.66666667  
0.25000000 0.50000000 0.66666667  
0.25000000 1.00000000 0.66666667  
0.50000000 0.00000000 0.66666667  
0.50000000 0.25000000 0.33333333  
0.50000000 0.75000000 0.00000000  
0.50000000 0.75000000 0.66666667  
0.50000000 1.00000000 0.33333333  
0.50000000 0.75000000 0.33333333  
0.75000000 0.00000000 0.00000000  
0.75000000 0.25000000 0.66666667  
0.75000000 0.25000000 0.00000000  
0.75000000 0.25000000 0.33333333  
0.00000000 0.25000000 0.00000000  
0.00000000 0.50000000 0.00000000  
0.00000000 0.25000000 0.33333333  
0.00000000 0.50000000 0.33333333  
0.00000000 0.25000000 0.66666667  
0.25000000 0.50000000 0.00000000  
0.25000000 0.75000000 0.00000000  
0.25000000 0.75000000 0.33333333  
0.25000000 0.75000000 0.66666667  
0.25000000 0.50000000 0.33333333  
0.50000000 0.25000000 0.66666667  
0.50000000 0.00000000 0.00000000  
0.50000000 0.25000000 0.00000000  
0.50000000 0.50000000 0.00000000  
0.50000000 0.50000000 0.66666667  
0.50000000 0.50000000 0.33333333  
0.75000000 0.50000000 0.00000000  
0.75000000 0.50000000 0.33333333  
0.75000000 0.50000000 0.66666667  
0.75000000 0.75000000 0.00000000  
0.75000000 0.75000000 0.33333333  
0.75000000 0.75000000 0.66666667  
0.75000000 1.00000000 0.66666667  
0.75000000 1.00000000 0.33333333

B3 A<sub>0.75</sub>B<sub>0.25</sub>N POSCAR

A36 B12 N48

4.18

2.00000000 2.00000000 0.00000000  
 0.00000000 2.00000000 2.00000000  
 1.50000000 0.00000000 1.5000000

B A N

12 36 48

direct

0.75000000 0.00000000 0.66666667 B  
 0.00000000 0.50000000 0.00000000 B  
 0.25000000 0.75000000 1.00000000 B  
 0.50000000 0.25000000 0.00000000 B  
 0.50000000 0.75000000 1.00000000 B  
 0.00000000 0.50000000 0.33333333 B  
 0.25000000 0.75000000 0.33333333 B  
 0.25000000 0.75000000 0.66666667 B  
 0.50000000 0.75000000 0.66666667 B  
 0.75000000 0.50000000 0.33333333 B  
 0.75000000 0.75000000 0.33333333 B  
 0.75000000 0.75000000 0.66666667 B  
 0.00000000 0.00000000 0.00000000 A  
 0.25000000 0.00000000 0.00000000 A  
 0.50000000 0.00000000 0.00000000 A  
 0.75000000 0.00000000 0.00000000 A  
 0.00000000 0.00000000 0.33333333 A  
 0.00000000 0.00000000 0.66666667 A  
 0.25000000 0.00000000 0.33333333 A  
 0.25000000 0.00000000 0.66666667 A  
 0.50000000 0.00000000 0.33333333 A  
 0.50000000 0.00000000 0.66666667 A  
 0.75000000 0.00000000 0.33333333 A  
 0.00000000 0.25000000 0.00000000 A  
 0.00000000 0.75000000 1.00000000 A  
 0.25000000 0.25000000 0.00000000 A  
 0.25000000 0.50000000 0.00000000 A  
 0.50000000 0.50000000 0.00000000 A  
 0.75000000 0.25000000 0.00000000 A  
 0.75000000 0.50000000 0.00000000 A  
 0.75000000 0.75000000 0.00000000 A  
 0.00000000 0.25000000 0.33333333 A  
 0.00000000 0.75000000 0.33333333 A  
 0.00000000 0.25000000 0.66666667 A  
 0.00000000 0.50000000 0.66666667 A  
 0.00000000 0.75000000 0.66666667 A  
 0.25000000 0.25000000 0.33333333 A  
 0.25000000 0.50000000 0.33333333 A  
 0.25000000 0.25000000 0.66666667 A  
 0.25000000 0.50000000 0.66666667 A  
 0.50000000 0.25000000 0.33333333 A  
 0.50000000 0.50000000 0.33333333 A  
 0.50000000 0.75000000 0.33333333 A  
 0.50000000 0.25000000 0.66666667 A  
 0.50000000 0.50000000 0.66666667 A  
 0.75000000 0.25000000 0.33333333 A  
 0.75000000 0.25000000 0.66666667 A  
 0.75000000 0.50000000 0.66666667 A  
 0.06250000 0.06250000 0.08333334 N

0.31250000 0.06250000 0.08333334 N  
0.56250000 0.06250000 0.08333334 N  
0.81250000 0.06250000 0.08333334 N  
0.06250000 0.06250000 0.41666667 N  
0.06250000 0.06250000 0.75000000 N  
0.31250000 0.06250000 0.41666667 N  
0.31250000 0.06250000 0.75000000 N  
0.56250000 0.06250000 0.41666667 N  
0.56250000 0.06250000 0.75000000 N  
0.81250000 0.06250000 0.41666667 N  
0.81250000 0.06250000 0.75000000 N  
0.06250000 0.31250000 0.08333334 N  
0.06250000 0.56250000 0.08333334 N  
0.06250000 0.81250000 0.08333334 N  
0.31250000 0.31250000 0.08333334 N  
0.31250000 0.56250000 0.08333334 N  
0.31250000 0.81250000 0.08333334 N  
0.56250000 0.31250000 0.08333334 N  
0.56250000 0.56250000 0.08333334 N  
0.56250000 0.81250000 0.08333334 N  
0.81250000 0.31250000 0.08333334 N  
0.81250000 0.56250000 0.08333334 N  
0.81250000 0.81250000 0.08333334 N  
0.06250000 0.31250000 0.41666667 N  
0.06250000 0.56250000 0.41666667 N  
0.06250000 0.81250000 0.41666667 N  
0.06250000 0.31250000 0.75000000 N  
0.06250000 0.56250000 0.75000000 N  
0.06250000 0.81250000 0.75000000 N  
0.31250000 0.31250000 0.41666667 N  
0.31250000 0.56250000 0.41666667 N  
0.31250000 0.81250000 0.41666667 N  
0.31250000 0.31250000 0.75000000 N  
0.31250000 0.56250000 0.75000000 N  
0.31250000 0.81250000 0.75000000 N  
0.56250000 0.31250000 0.41666667 N  
0.56250000 0.56250000 0.41666667 N  
0.56250000 0.81250000 0.41666667 N  
0.56250000 0.31250000 0.75000000 N  
0.56250000 0.56250000 0.75000000 N  
0.56250000 0.81250000 0.75000000 N  
0.81250000 0.31250000 0.41666667 N  
0.81250000 0.56250000 0.41666667 N  
0.81250000 0.81250000 0.41666667 N  
0.81250000 0.31250000 0.75000000 N  
0.81250000 0.56250000 0.75000000 N  
0.81250000 0.81250000 0.75000000 N

B4 A<sub>0.25</sub>B<sub>0.75</sub>N POSCAR

A12 B36 N48

4.0

-3.50000000 0.86602500 0.00000000  
 2.50000000 -2.59807500 0.00000000  
 0.00000000 0.00000000 4.89897900

A B N

12 36 48

direct

0.16666675 0.83333325 1.00000000 A  
 0.79166675 0.70833325 1.00000000 A  
 0.66666675 0.33333325 0.33333333 A  
 0.29166675 0.20833325 0.33333333 A  
 0.16666675 0.83333325 0.66666667 A  
 0.79166675 0.70833325 0.66666667 A  
 0.58333325 0.41666675 0.50000000 A  
 0.20833325 0.29166675 0.50000000 A  
 0.83333325 0.16666675 0.50000000 A  
 0.08333325 0.91666675 0.50000000 A  
 0.95833325 0.54166675 0.83333333 A  
 0.83333325 0.16666675 0.83333333 A  
 0.41666675 0.58333325 1.00000000 B  
 0.04166675 0.45833325 1.00000000 B  
 0.66666675 0.33333325 1.00000000 B  
 0.29166675 0.20833325 1.00000000 B  
 0.91666675 0.08333325 1.00000000 B  
 0.54166675 0.95833325 1.00000000 B  
 0.41666675 0.58333325 0.33333333 B  
 0.04166675 0.45833325 0.33333333 B  
 0.91666675 0.08333325 0.33333333 B  
 0.54166675 0.95833325 0.33333333 B  
 0.16666675 0.83333325 0.33333333 B  
 0.79166675 0.70833325 0.33333333 B  
 0.41666675 0.58333325 0.66666667 B  
 0.04166675 0.45833325 0.66666667 B  
 0.66666675 0.33333325 0.66666667 B  
 0.29166675 0.20833325 0.66666667 B  
 0.91666675 0.08333325 0.66666667 B  
 0.54166675 0.95833325 0.66666667 B  
 0.33333325 0.66666675 0.16666667 B  
 0.95833325 0.54166675 0.16666667 B  
 0.58333325 0.41666675 0.16666667 B  
 0.20833325 0.29166675 0.16666667 B  
 0.83333325 0.16666675 0.16666667 B  
 0.45833325 0.04166675 0.16666667 B  
 0.08333325 0.91666675 0.16666667 B  
 0.70833325 0.79166675 0.16666667 B  
 0.33333325 0.66666675 0.50000000 B  
 0.95833325 0.54166675 0.50000000 B  
 0.45833325 0.04166675 0.50000000 B  
 0.70833325 0.79166675 0.50000000 B  
 0.33333325 0.66666675 0.83333333 B  
 0.58333325 0.41666675 0.83333333 B  
 0.20833325 0.29166675 0.83333333 B  
 0.45833325 0.04166675 0.83333333 B  
 0.08333325 0.91666675 0.83333333 B  
 0.70833325 0.79166675 0.83333333 B  
 0.41666675 0.58333325 0.12666667 N

0.04166675 0.45833325 0.12666667 N  
0.66666675 0.33333325 0.12666667 N  
0.29166675 0.20833325 0.12666667 N  
0.91666675 0.08333325 0.12666667 N  
0.54166675 0.95833325 0.12666667 N  
0.16666675 0.83333325 0.12666667 N  
0.79166675 0.70833325 0.12666667 N  
0.41666675 0.58333325 0.46000000 N  
0.04166675 0.45833325 0.46000000 N  
0.66666675 0.33333325 0.46000000 N  
0.29166675 0.20833325 0.46000000 N  
0.91666675 0.08333325 0.46000000 N  
0.54166675 0.95833325 0.46000000 N  
0.16666675 0.83333325 0.46000000 N  
0.79166675 0.70833325 0.46000000 N  
0.41666675 0.58333325 0.79333333 N  
0.04166675 0.45833325 0.79333333 N  
0.66666675 0.33333325 0.79333333 N  
0.29166675 0.20833325 0.79333333 N  
0.91666675 0.08333325 0.79333333 N  
0.54166675 0.95833325 0.79333333 N  
0.16666675 0.83333325 0.79333333 N  
0.79166675 0.70833325 0.79333333 N  
0.33333325 0.66666675 0.29333333 N  
0.95833325 0.54166675 0.29333333 N  
0.58333325 0.41666675 0.29333333 N  
0.20833325 0.29166675 0.29333333 N  
0.83333325 0.16666675 0.29333333 N  
0.45833325 0.04166675 0.29333333 N  
0.08333325 0.91666675 0.29333333 N  
0.70833325 0.79166675 0.29333333 N  
0.33333325 0.66666675 0.62666667 N  
0.95833325 0.54166675 0.62666667 N  
0.58333325 0.41666675 0.62666667 N  
0.20833325 0.29166675 0.62666667 N  
0.83333325 0.16666675 0.62666667 N  
0.45833325 0.04166675 0.62666667 N  
0.08333325 0.91666675 0.62666667 N  
0.70833325 0.79166675 0.62666667 N  
0.33333325 0.66666675 0.96000000 N  
0.95833325 0.54166675 0.96000000 N  
0.58333325 0.41666675 0.96000000 N  
0.20833325 0.29166675 0.96000000 N  
0.83333325 0.16666675 0.96000000 N  
0.45833325 0.04166675 0.96000000 N  
0.08333325 0.91666675 0.96000000 N  
0.70833325 0.79166675 0.96000000 N

B4 A<sub>0.50</sub>B<sub>0.50</sub>N POSCAR

A24 B24 N48

4.0

-3.50000000 0.86602500 0.00000000  
 2.50000000 -2.59807500 0.00000000  
 0.00000000 0.00000000 4.89897900

A B N

24 24 48

direct

0.66666675 0.33333325 1.00000000 A  
 0.29166675 0.20833325 1.00000000 A  
 0.91666675 0.08333325 1.00000000 A  
 0.79166675 0.70833325 1.00000000 A  
 0.41666675 0.58333325 0.33333333 A  
 0.04166675 0.45833325 0.33333333 A  
 0.91666675 0.08333325 0.33333333 A  
 0.54166675 0.95833325 0.33333333 A  
 0.16666675 0.83333325 0.33333333 A  
 0.79166675 0.70833325 0.33333333 A  
 0.04166675 0.45833325 0.66666667 A  
 0.29166675 0.20833325 0.66666667 A  
 0.91666675 0.08333325 0.66666667 A  
 0.16666675 0.83333325 0.66666667 A  
 0.33333325 0.66666675 0.16666667 A  
 0.58333325 0.41666675 0.16666667 A  
 0.70833325 0.79166675 0.16666667 A  
 0.33333325 0.66666675 0.50000000 A  
 0.58333325 0.41666675 0.50000000 A  
 0.20833325 0.29166675 0.50000000 A  
 0.08333325 0.91666675 0.50000000 A  
 0.70833325 0.79166675 0.50000000 A  
 0.83333325 0.16666675 0.83333333 A  
 0.70833325 0.79166675 0.83333333 A  
 0.41666675 0.58333325 1.00000000 B  
 0.04166675 0.45833325 1.00000000 B  
 0.54166675 0.95833325 1.00000000 B  
 0.16666675 0.83333325 1.00000000 B  
 0.66666675 0.33333325 0.33333333 B  
 0.29166675 0.20833325 0.33333333 B  
 0.41666675 0.58333325 0.66666667 B  
 0.66666675 0.33333325 0.66666667 B  
 0.54166675 0.95833325 0.66666667 B  
 0.79166675 0.70833325 0.66666667 B  
 0.95833325 0.54166675 0.16666667 B  
 0.20833325 0.29166675 0.16666667 B  
 0.83333325 0.16666675 0.16666667 B  
 0.45833325 0.04166675 0.16666667 B  
 0.08333325 0.91666675 0.16666667 B  
 0.95833325 0.54166675 0.50000000 B  
 0.83333325 0.16666675 0.50000000 B  
 0.45833325 0.04166675 0.50000000 B  
 0.33333325 0.66666675 0.83333333 B  
 0.95833325 0.54166675 0.83333333 B  
 0.58333325 0.41666675 0.83333333 B  
 0.20833325 0.29166675 0.83333333 B  
 0.45833325 0.04166675 0.83333333 B  
 0.08333325 0.91666675 0.83333333 B  
 0.41666675 0.58333325 0.12666667 N

0.04166675 0.45833325 0.12666667 N  
0.66666675 0.33333325 0.12666667 N  
0.29166675 0.20833325 0.12666667 N  
0.91666675 0.08333325 0.12666667 N  
0.54166675 0.95833325 0.12666667 N  
0.16666675 0.83333325 0.12666667 N  
0.79166675 0.70833325 0.12666667 N  
0.41666675 0.58333325 0.46000000 N  
0.04166675 0.45833325 0.46000000 N  
0.66666675 0.33333325 0.46000000 N  
0.29166675 0.20833325 0.46000000 N  
0.91666675 0.08333325 0.46000000 N  
0.54166675 0.95833325 0.46000000 N  
0.16666675 0.83333325 0.46000000 N  
0.79166675 0.70833325 0.46000000 N  
0.41666675 0.58333325 0.79333333 N  
0.04166675 0.45833325 0.79333333 N  
0.66666675 0.33333325 0.79333333 N  
0.29166675 0.20833325 0.79333333 N  
0.91666675 0.08333325 0.79333333 N  
0.54166675 0.95833325 0.79333333 N  
0.16666675 0.83333325 0.79333333 N  
0.79166675 0.70833325 0.79333333 N  
0.33333325 0.66666675 0.29333333 N  
0.95833325 0.54166675 0.29333333 N  
0.58333325 0.41666675 0.29333333 N  
0.20833325 0.29166675 0.29333333 N  
0.83333325 0.16666675 0.29333333 N  
0.45833325 0.04166675 0.29333333 N  
0.08333325 0.91666675 0.29333333 N  
0.70833325 0.79166675 0.29333333 N  
0.33333325 0.66666675 0.62666667 N  
0.95833325 0.54166675 0.62666667 N  
0.58333325 0.41666675 0.62666667 N  
0.20833325 0.29166675 0.62666667 N  
0.83333325 0.16666675 0.62666667 N  
0.45833325 0.04166675 0.62666667 N  
0.08333325 0.91666675 0.62666667 N  
0.70833325 0.79166675 0.62666667 N  
0.33333325 0.66666675 0.96000000 N  
0.95833325 0.54166675 0.96000000 N  
0.58333325 0.41666675 0.96000000 N  
0.20833325 0.29166675 0.96000000 N  
0.83333325 0.16666675 0.96000000 N  
0.45833325 0.04166675 0.96000000 N  
0.08333325 0.91666675 0.96000000 N  
0.70833325 0.79166675 0.96000000 N

B4 A<sub>0.75</sub>B<sub>0.25</sub>N POSCAR

B12 A36 N48

4.0

-3.50000000 0.86602500 0.00000000  
 2.50000000 -2.59807500 0.00000000  
 0.00000000 0.00000000 4.89897900

B A N

12 36 48

direct

0.16666675 0.83333325 1.00000000 B  
 0.79166675 0.70833325 1.00000000 B  
 0.66666675 0.33333325 0.33333333 B  
 0.29166675 0.20833325 0.33333333 B  
 0.16666675 0.83333325 0.66666667 B  
 0.79166675 0.70833325 0.66666667 B  
 0.58333325 0.41666675 0.50000000 B  
 0.20833325 0.29166675 0.50000000 B  
 0.83333325 0.16666675 0.50000000 B  
 0.08333325 0.91666675 0.50000000 B  
 0.95833325 0.54166675 0.83333333 B  
 0.83333325 0.16666675 0.83333333 B  
 0.41666675 0.58333325 1.00000000 A  
 0.04166675 0.45833325 1.00000000 A  
 0.66666675 0.33333325 1.00000000 A  
 0.29166675 0.20833325 1.00000000 A  
 0.91666675 0.08333325 1.00000000 A  
 0.54166675 0.95833325 1.00000000 A  
 0.41666675 0.58333325 0.33333333 A  
 0.04166675 0.45833325 0.33333333 A  
 0.91666675 0.08333325 0.33333333 A  
 0.54166675 0.95833325 0.33333333 A  
 0.16666675 0.83333325 0.33333333 A  
 0.79166675 0.70833325 0.33333333 A  
 0.41666675 0.58333325 0.66666667 A  
 0.04166675 0.45833325 0.66666667 A  
 0.66666675 0.33333325 0.66666667 A  
 0.29166675 0.20833325 0.66666667 A  
 0.91666675 0.08333325 0.66666667 A  
 0.54166675 0.95833325 0.66666667 A  
 0.33333325 0.66666675 0.16666667 A  
 0.95833325 0.54166675 0.16666667 A  
 0.58333325 0.41666675 0.16666667 A  
 0.20833325 0.29166675 0.16666667 A  
 0.83333325 0.16666675 0.16666667 A  
 0.45833325 0.04166675 0.16666667 A  
 0.08333325 0.91666675 0.16666667 A  
 0.70833325 0.79166675 0.16666667 A  
 0.33333325 0.66666675 0.50000000 A  
 0.95833325 0.54166675 0.50000000 A  
 0.45833325 0.04166675 0.50000000 A  
 0.70833325 0.79166675 0.50000000 A  
 0.33333325 0.66666675 0.83333333 A  
 0.58333325 0.41666675 0.83333333 A  
 0.20833325 0.29166675 0.83333333 A  
 0.45833325 0.04166675 0.83333333 A  
 0.08333325 0.91666675 0.83333333 A  
 0.70833325 0.79166675 0.83333333 A  
 0.41666675 0.58333325 0.12666667 N

0.04166675 0.45833325 0.12666667 N  
0.66666675 0.33333325 0.12666667 N  
0.29166675 0.20833325 0.12666667 N  
0.91666675 0.08333325 0.12666667 N  
0.54166675 0.95833325 0.12666667 N  
0.16666675 0.83333325 0.12666667 N  
0.79166675 0.70833325 0.12666667 N  
0.41666675 0.58333325 0.46000000 N  
0.04166675 0.45833325 0.46000000 N  
0.66666675 0.33333325 0.46000000 N  
0.29166675 0.20833325 0.46000000 N  
0.91666675 0.08333325 0.46000000 N  
0.54166675 0.95833325 0.46000000 N  
0.16666675 0.83333325 0.46000000 N  
0.79166675 0.70833325 0.46000000 N  
0.41666675 0.58333325 0.79333333 N  
0.04166675 0.45833325 0.79333333 N  
0.66666675 0.33333325 0.79333333 N  
0.29166675 0.20833325 0.79333333 N  
0.91666675 0.08333325 0.79333333 N  
0.54166675 0.95833325 0.79333333 N  
0.16666675 0.83333325 0.79333333 N  
0.79166675 0.70833325 0.79333333 N  
0.33333325 0.66666675 0.29333333 N  
0.95833325 0.54166675 0.29333333 N  
0.58333325 0.41666675 0.29333333 N  
0.20833325 0.29166675 0.29333333 N  
0.83333325 0.16666675 0.29333333 N  
0.45833325 0.04166675 0.29333333 N  
0.08333325 0.91666675 0.29333333 N  
0.70833325 0.79166675 0.29333333 N  
0.33333325 0.66666675 0.62666667 N  
0.95833325 0.54166675 0.62666667 N  
0.58333325 0.41666675 0.62666667 N  
0.20833325 0.29166675 0.62666667 N  
0.83333325 0.16666675 0.62666667 N  
0.45833325 0.04166675 0.62666667 N  
0.08333325 0.91666675 0.62666667 N  
0.70833325 0.79166675 0.62666667 N  
0.33333325 0.66666675 0.96000000 N  
0.95833325 0.54166675 0.96000000 N  
0.58333325 0.41666675 0.96000000 N  
0.20833325 0.29166675 0.96000000 N  
0.83333325 0.16666675 0.96000000 N  
0.45833325 0.04166675 0.96000000 N  
0.08333325 0.91666675 0.96000000 N  
0.70833325 0.79166675 0.96000000 N